Localisation précise par moyens spatiaux

LEO POD using GPS

Adrian Jäggi
Astronomical Institute
University of Bern

Low Earth Orbiters (LEOs)

GRACE

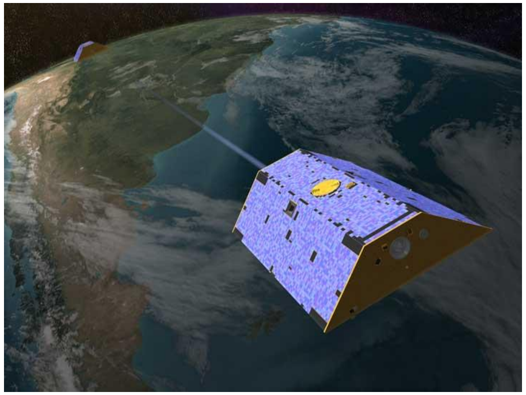

Gravity **R**ecovery **A**nd **C**limate **E**xperiment

GOCE

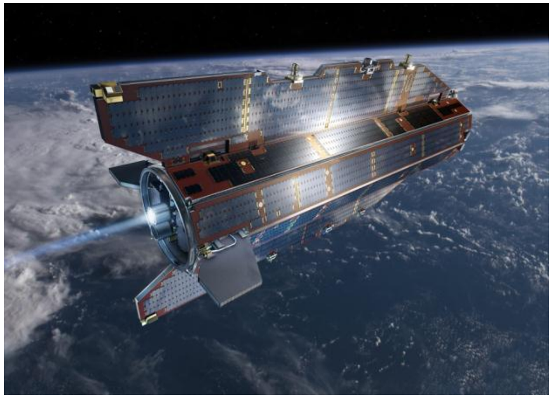

Gravity and steady-state **O**cean **C**irculation **E**xplorer

TanDEM-X

TerraSAR-X **a**dd-o**n** for **D**igital **E**levation **M**easurement

Of course, there are many more missions equipped with GPS receivers

Jason

Jason-2

MetOp-A

Icesat

COSMIC

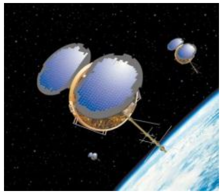

LEO positioning

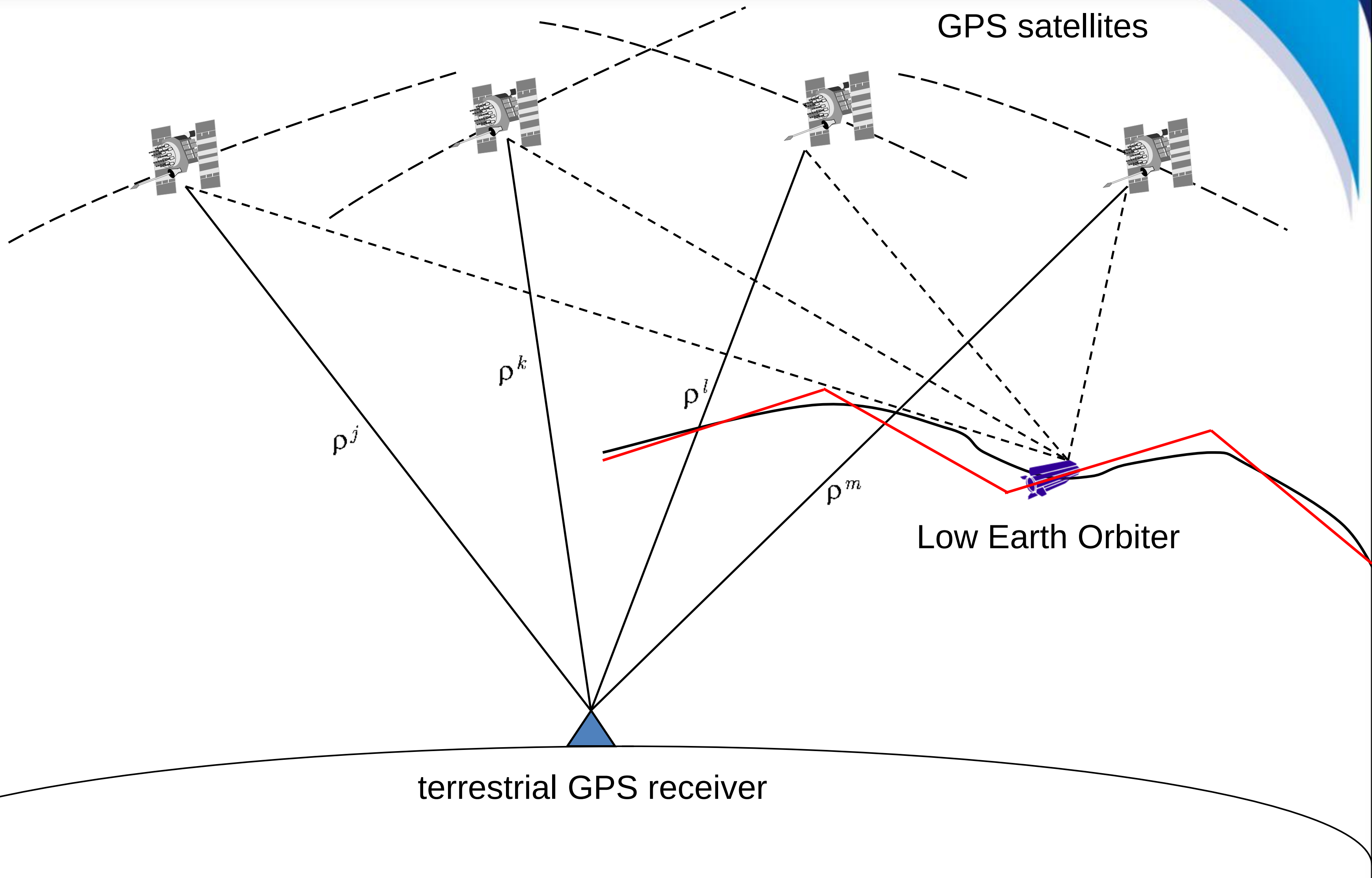

Least-squares adjustment

linearized observation equations:

$$\Delta\mathbf{l} = \mathbf{A}\cdot\Delta\mathbf{x} - \mathbf{v} \quad \text{with} \quad \mathbf{P} = \sigma_o^{\,2}\mathbf{C}^{-1}$$

covariance matrix:

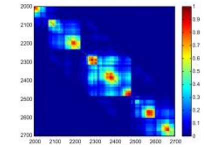

observed-minus-compu

$$\Delta\mathbf{l} = \begin{pmatrix} l_1' - F_1(\mathbf{x}_0) \\ l_2' - F_2(\mathbf{x}_0) \\ \vdots \\ l_n' - F_n(\mathbf{x}_0) \end{pmatrix}$$

pseudo-observations:

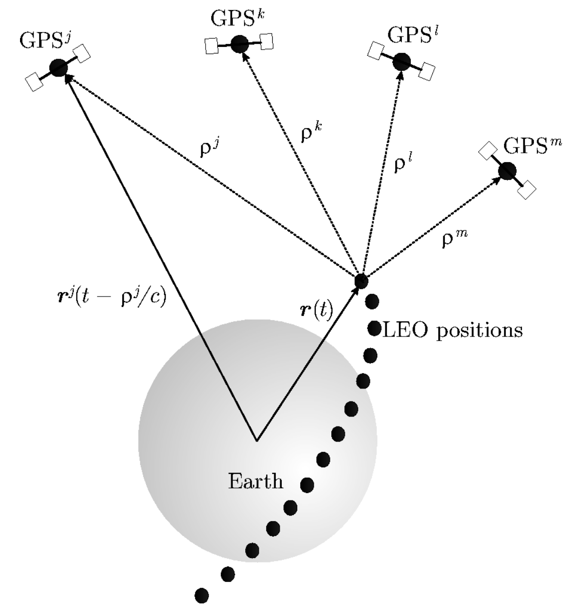

unknown parameters:

$$\Delta\mathbf{x} = \begin{pmatrix} \Delta c_{00} \\ \vdots \\ \Delta c_{nm} \\ \Delta s_{nm} \end{pmatrix}$$

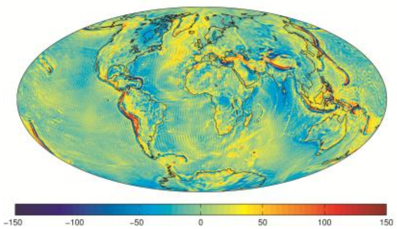

syst

v

$$\Delta\mathbf{x} = \left(\mathbf{A}^T\mathbf{P}\mathbf{A}\right)^{-1}\mathbf{A}^T\mathbf{P}\Delta\mathbf{l}$$

Geometric distance LEO-GPS

Geometric distance ρ_{leo}^{k} is given by:

$$\rho_{leo}^{k} = \left| \boldsymbol{r}_{leo}(t_{leo}) - \boldsymbol{r}^{k}(t_{leo} - \tau_{leo}^{k}) \right|$$

$\boldsymbol{r}_{leo}$ Inertial position of LEO antenna phase center at reception time

$\boldsymbol{r}^{k}$ Inertial position of GPS antenna phase center of satellite k at emission time

τ_{leo}^{k} Signal traveling time between the two phase center positions

Different ways to represent $\boldsymbol{r}_{leo}$:

- **Kinematic** orbit representation
- **Dynamic** or **reduced-dynamic** orbit representation

Kinematic orbit representation

Satellite position $\boldsymbol{r}_{leo}(t_{leo})$ (in inertial frame) is given by:

$$\boldsymbol{r}_{leo}(t_{leo}) = \boldsymbol{R}(t_{leo}) \cdot (\boldsymbol{r}_{leo,e,0}(t_{leo}) + \delta\boldsymbol{r}_{leo,e,ant}(t_{leo}))$$

$\boldsymbol{R}$	Transformation matrix from Earth-fixed to inertial frame
$\boldsymbol{r}_{leo,e,0}$	LEO center of mass position in Earth-fixed frame
$\delta\boldsymbol{r}_{leo,e,ant}$	LEO antenna phase center offset in Earth-fixed frame

Kinematic positions $\boldsymbol{r}_{leo,e,0}$ are estimated for each **measurement epoch**:

- Measurement epochs **need not** to be identical with nominal epochs
- Positions are **independent** of models describing the LEO dynamics
  Velocities cannot be provided in a strict sense

Kinematic orbit representation

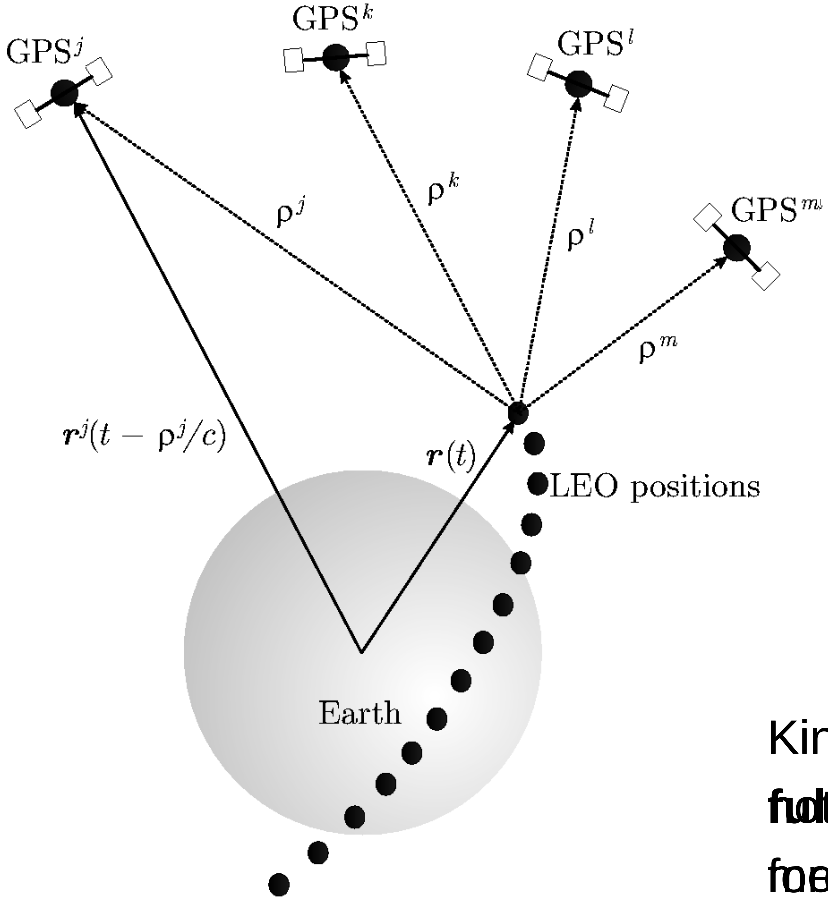

A kinematic orbit is an ephemeris at **discrete** measurement epochs

Kinematic positions are **fully independent** from the force models used for LEO orbit determination

Kinematic positions are uncorrelated if phase measurements are used (due to ambiguities)

Kinematic orbit determination

Measurement epochs (in GPS time)

Positions (km) (Earth-fixed)

Clock correction to nominal epoch (μs), e.g., to epoch 00:00:03

```
*  2009 11  2  0  0  0.80678020
PL15  -390.612059  6623.987679  73.104149 193219.797196
*  2009 11  2  0  0  1.80678020
PL15  -389.240315  6624.166512  65.402457 193219.799413
*  2009 11  2  0  0  2.80678020
PL15  -387.868014  6624.336133  57.700679 193219.801634
*  2009 11  2  0  0  3.80678020
PL15  -386.495163  6624.496541  49.998817 193219.803855
*  2009 11  2  0  0  4.80678019
PL15  -385.121760  6624.647724  42.296889 193219.806059
*  2009 11  2  0  0  5.80678019
PL15  -383.747819  6624.789703  34.594896 193219.808280
*  2009 11  2  0  0  6.80678019
PL15  -382.373332  6624.922464  26.892861 193219.810495
*  2009 11  2  0  0  7.80678019
PL15  -380.998306  6625.046003  19.190792 193219.812692
*  2009 11  2  0  0  8.80678019
PL15  -379.622745  6625.160329  11.488692 193219.814899
*  2009 11  2  0  0  9.80678018
PL15  -378.246651  6625.265448   3.786580 193219.817123
```

Excerpt of kinematic GOCE positions at begin of 2 Nov, 2009

GO_CONS_SST_PKI_2__20091101T235945_20091102T235944_0001 Times in UTC

Dynamic orbit representation

Satellite position $\boldsymbol{r}_{leo}(t_{leo})$ (in inertial frame) is given by:

$$\boldsymbol{r}_{leo}(t_{leo}) = \boldsymbol{r}_{leo,0}(t_{leo}; a, e, i, \Omega, \omega, u_0; Q_1, ..., Q_d) + \delta\boldsymbol{r}_{leo,ant}(t_{leo})$$

$\boldsymbol{r}_{leo,0}$	LEO center of mass position
$\delta\boldsymbol{r}_{leo,ant}$	LEO antenna phase center offset
$a, e, i, \Omega, \omega, u_0$	LEO initial osculating orbital elements
$Q_1, ..., Q_d$	LEO dynamical parameters

Satellite trajectory $\boldsymbol{r}_{leo,0}$ is a particular solution of an **equation of motion**

- One set of **initial conditions** (orbital elements) is estimated per arc
  Dynamical parameters of the force model on request

Dynamic orbit representation

Equation of motion (in inertial frame) is given by:

$$\ddot{\boldsymbol{r}} = -GM\frac{\boldsymbol{r}}{r^3} + \boldsymbol{f}_1(t, \boldsymbol{r}, \dot{\boldsymbol{r}}, Q_1, ..., Q_d)$$

with initial conditions

$$\boldsymbol{r}(t_0) = \boldsymbol{r}(a, e, i, \Omega, \omega, u_0; t_0)$$
$$\dot{\boldsymbol{r}}(t_0) = \dot{\boldsymbol{r}}(a, e, i, \Omega, \omega, u_0; t_0)$$

The **acceleration** $\boldsymbol{f}_1$ consists of **gravitational** and **non-gravitational** perturbations taken into account to model the satellite trajectory. Unknown parameters $Q_1, ..., Q_d$ of force models may appear in the equation of motion together with deterministic (known) accelerations given by analytical models.

Osculating orbital elements

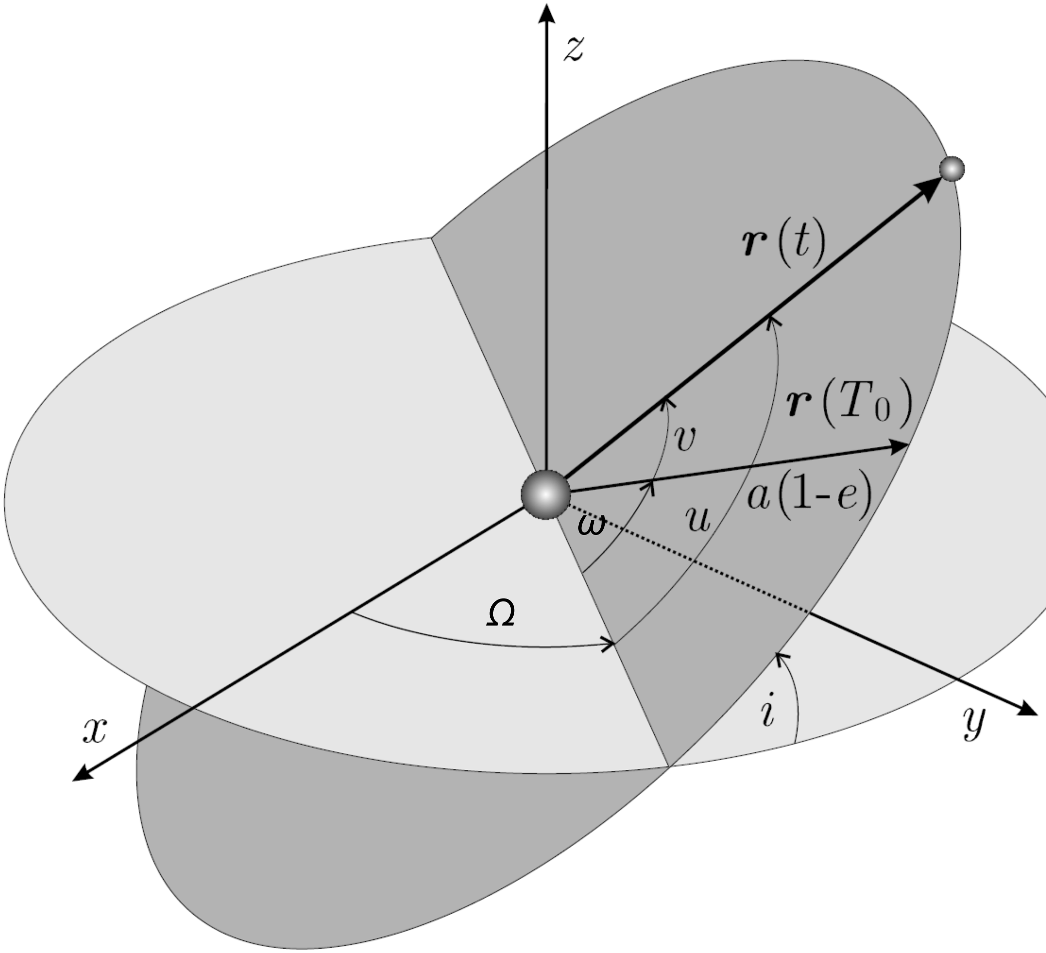

Osculating orbital elements of GOCE

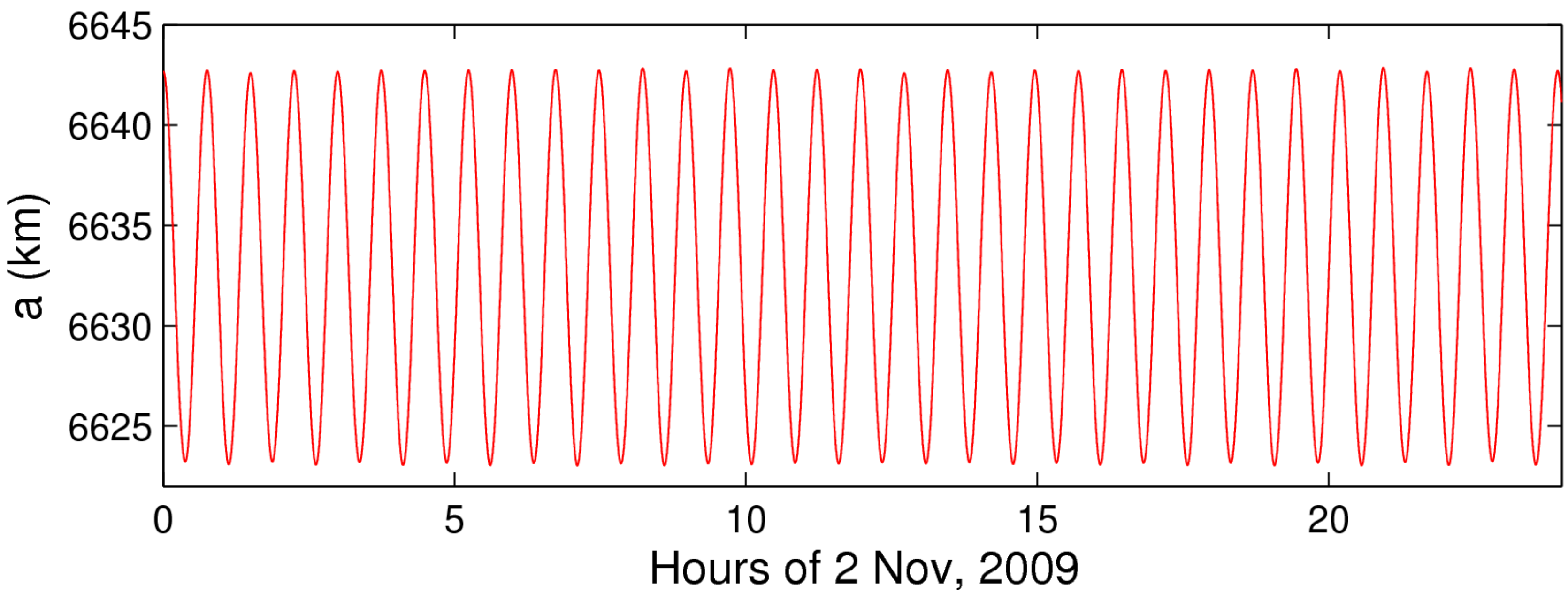

Semi-major axis:

Twice-per-revolution variations of about ±10 km around the mean semi-major axis of 6632.9km, which corresponds to a mean altitude of 254.9 km

Osculating orbital elements of GOCE

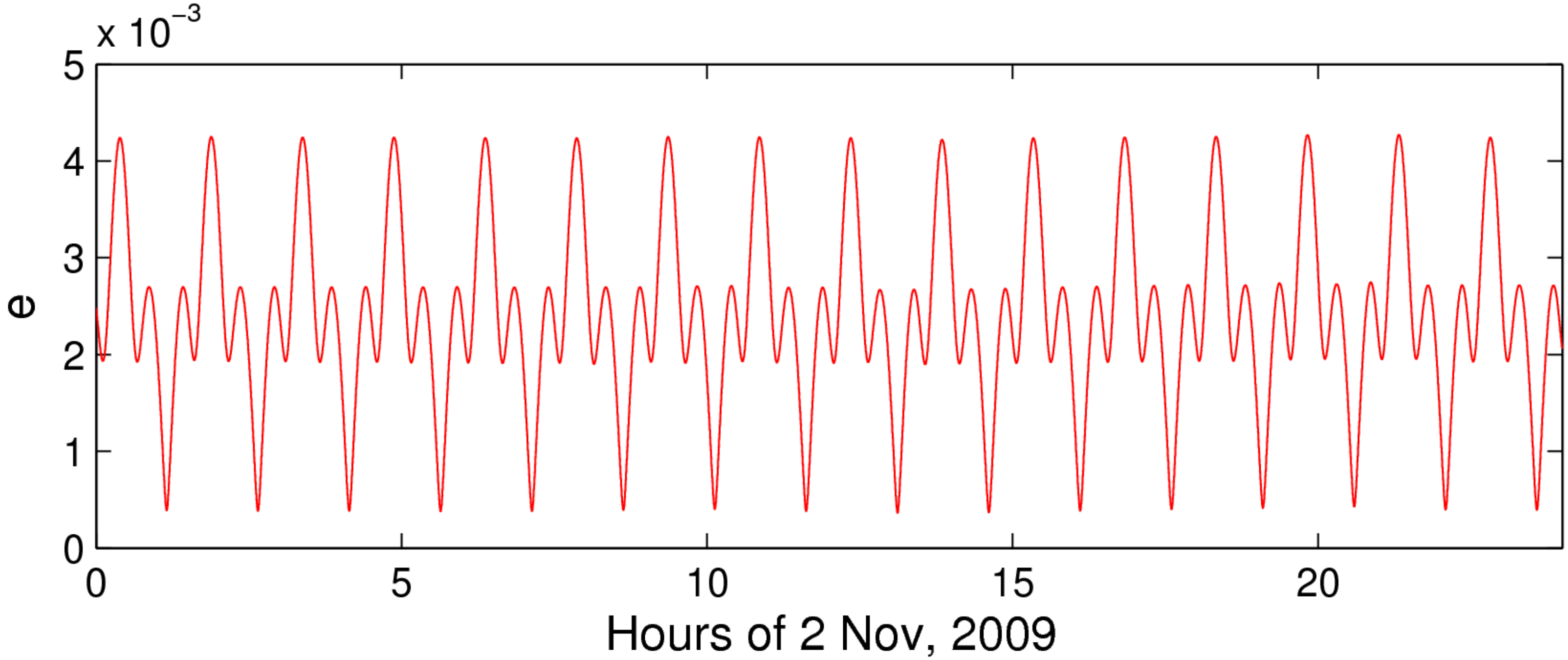

Numerical eccentricity:

Small, short-periodic variations around the mean value of about 0.0025, i.e., the orbit is close to circular

Osculating orbital elements of GOCE

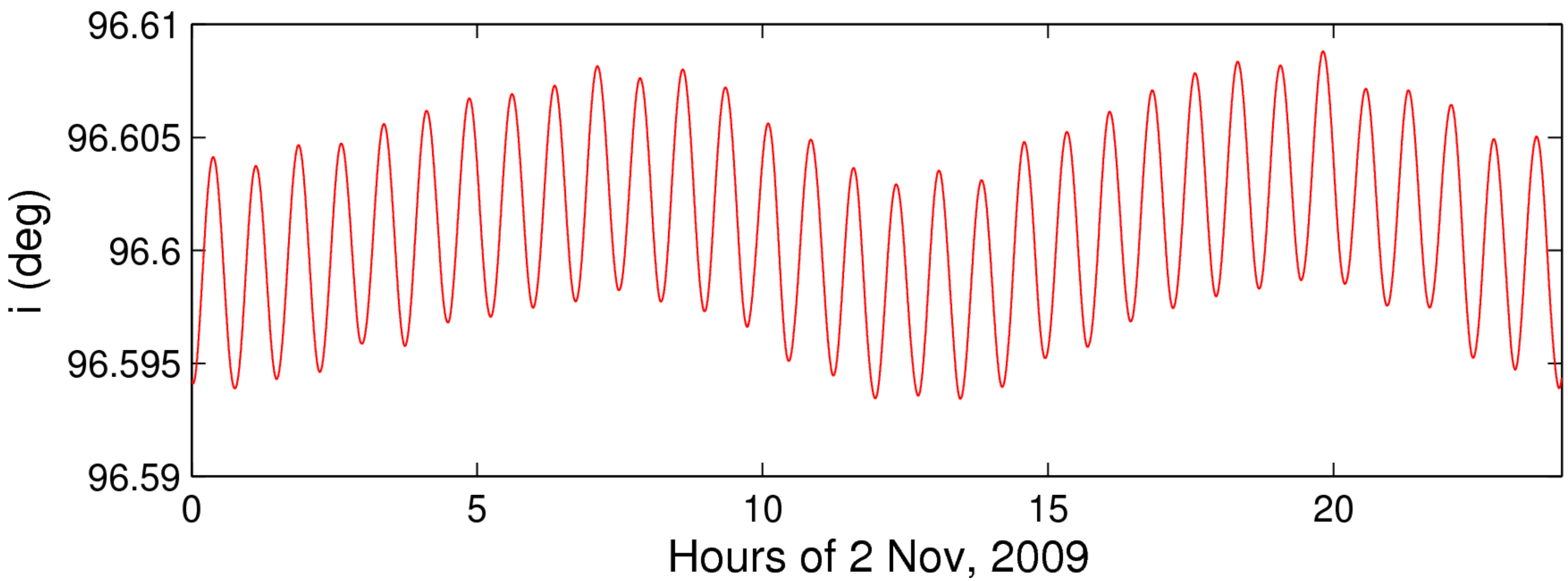

Inclination:

Twice-per-revolution and longer variations around the mean inclination of about 96.6° (sun-synchronous orbit)

Osculating orbital elements of GOCE

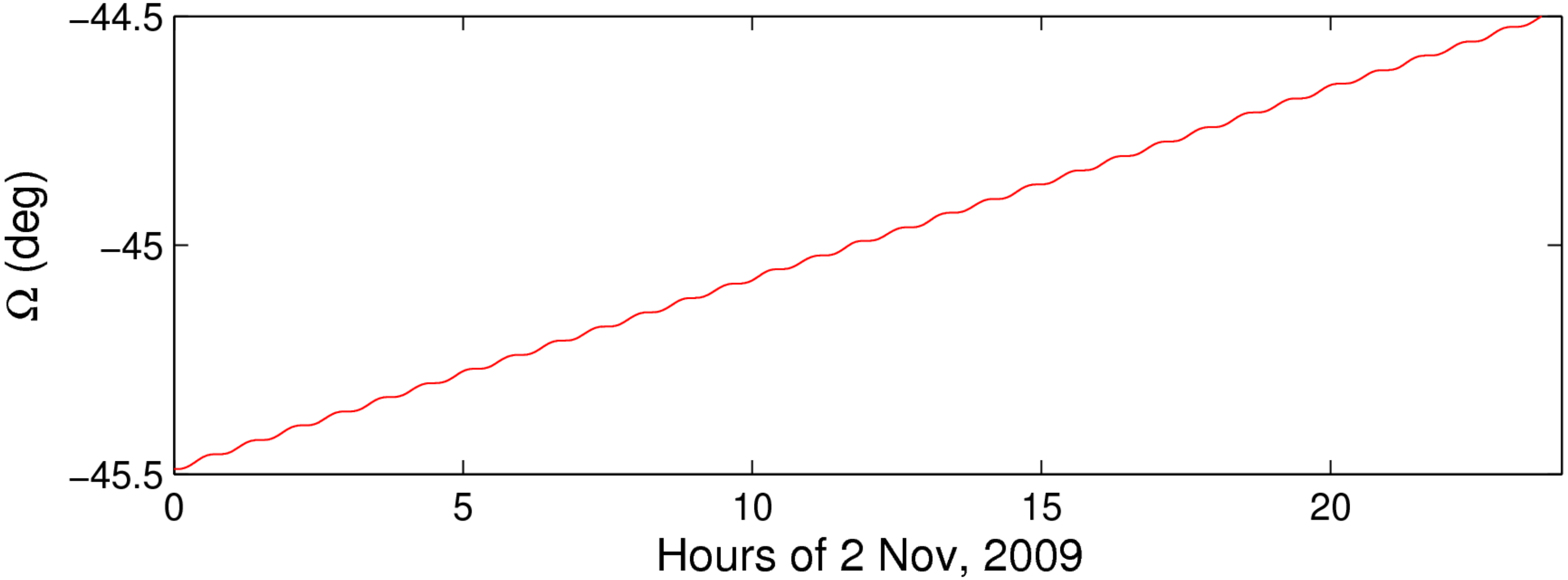

Right ascension of ascending node:

Twice-per-revolution variations and linear drift of about +1°/day (360°/365days) due to the sun-synchronous orbit

Dynamic orbit representation

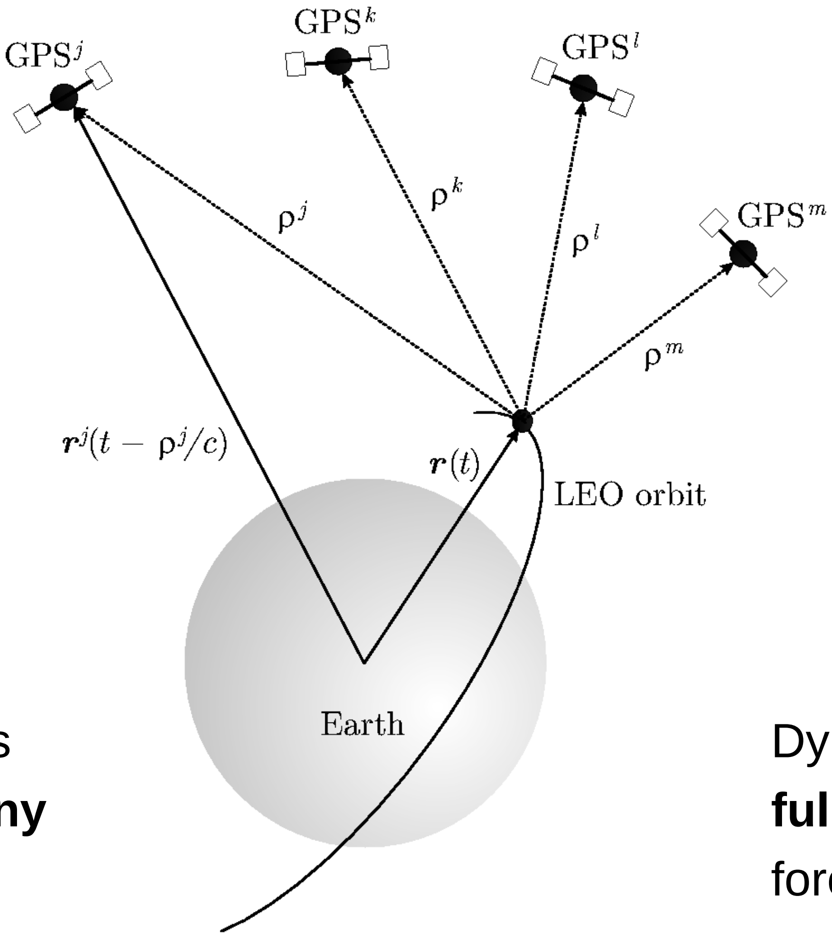

Dynamic orbit positions may be computed at **any epoch** within the arc

Dynamic positions are **fully dependent** on the force models used, e.g., on the gravity field model

Reduced-dynamic orbit representation

Equation of motion (in inertial frame) is given by:

$$\ddot{\boldsymbol{r}} = -GM\frac{\boldsymbol{r}}{r^3} + \boldsymbol{f}_1(t, \boldsymbol{r}, \dot{\boldsymbol{r}}, Q_1, ..., Q_d, P_1, ..., P_s)$$

$P_1, ..., P_s$ Pseudo-stochastic parameters

Pseudo-stochastic parameters are:

- additional empirical parameters characterized by a priori known **statistical properties**, e.g., by expectation values and a priori variances
- useful to **compensate** for deficiencies in dynamic models, e.g., deficiencies in models describing non-gravitational accelerations
- often set up as **piecewise constant accelerations** to ensure that satellite trajectories are continuous and differentiable at any epoch

Reduced-dynamic orbit representation

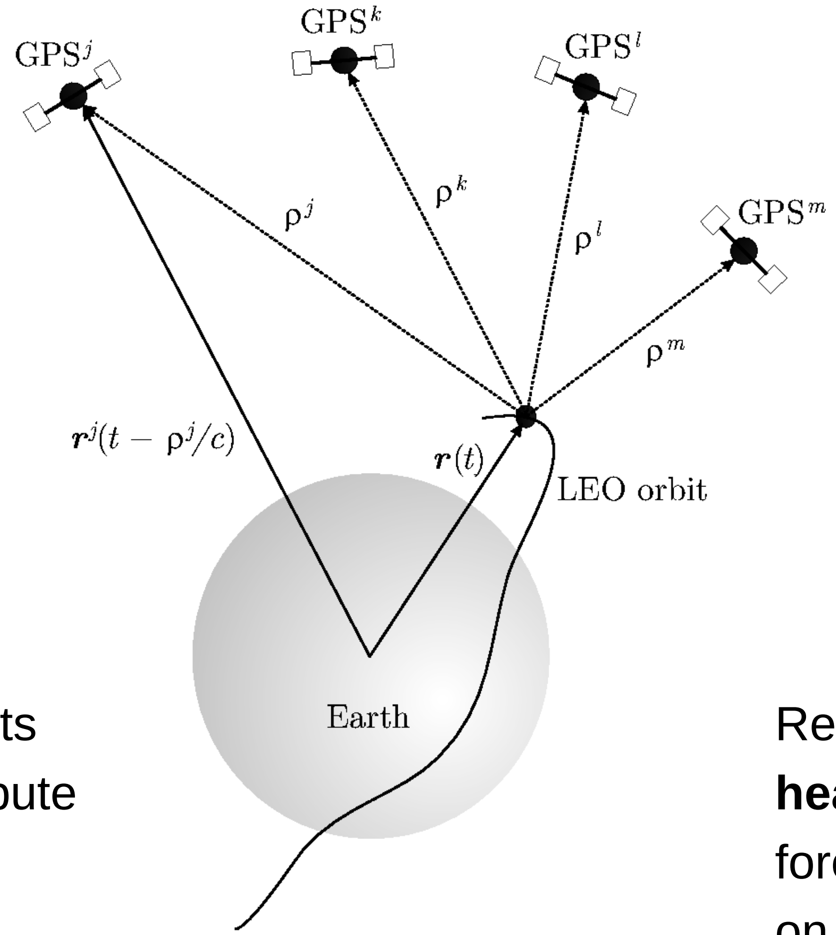

Reduced-dynamic orbits are well suited to compute LEO orbits of **highest quality**

Reduced-dynamic orbits **heavily depend** on the force models used, e.g., on the gravity field model

Perturbations acting on LEOs

Perturbation	Acceleration (m/s²)
Main term of Earth‘s gravity field	8.42
Oblateness	0.015
Atmospheric drag	0.00000079
Higher terms of Earth‘s gravity field	0.00025
Lunar attraction	0.0000054
Solar attraction	0.0000005
Direct radiation pressure	0.000000097
.	.

The orders of magnitude refer to:
- orbital altitude of 500 km
- area-to-mass ratio of 0.02 m^2/kg

Gravitational perturbations

$$V(r,\theta,\lambda) = \frac{GM}{R} \sum_{l=0}^{l_{\max}} \left(\frac{R}{r}\right)^{l+1} \sum_{m=0}^{l} \bar{P}_{lm}(\cos\theta) \cdot \left[\bar{C}_{lm} \cos(m\lambda) + \bar{S}_{lm} \sin(m\lambda) \right]$$

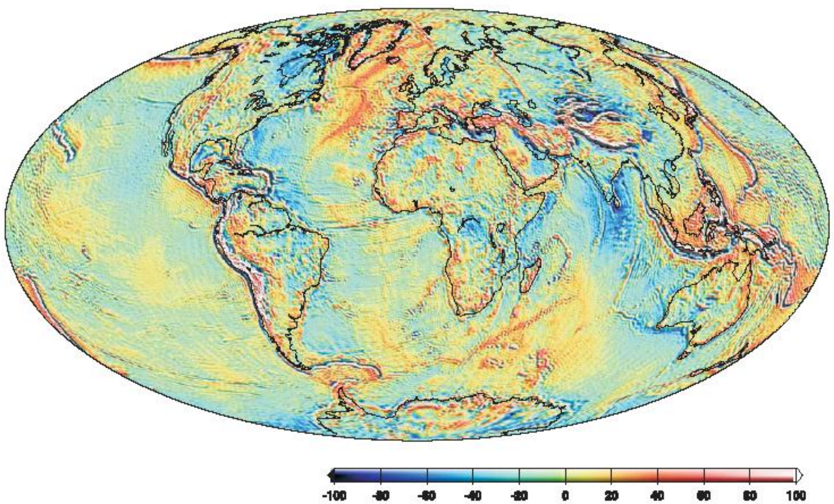

Gravity anomalies (in mgal)

CHAMP

GRACE

GOCE

l_{max}	# of coeff.	λ [km]
20	441	1000
100	10 201	200
200	40 401	100
250	63 001	80

λ … spatial (half) wavelength

Depending on the LEO orbital altitude, gravity field coefficients have to be taken into account up to different maximum degrees and orders for precise orbit determination, e.g., at least up to about degree and order 160 for GOCE POD

Partial derivatives

Orbit improvement ($\boldsymbol{r}_0(t)$: numerically integrated **a priori orbit**):

$$\boldsymbol{r}(t) = \boldsymbol{r}_0(t) + \sum_{i=1}^{n} \frac{\partial \boldsymbol{r}_0}{\partial P_i}(t) \cdot (P_i - P_{0,i})$$

yields corrections to a priori parameter values $P_{0,i}$ by **least-squares**

Previously, for each parameter P_i the corresponding **variational equation**

$$\ddot{\boldsymbol{z}}_{P_i} = \boldsymbol{A}_0 \cdot \boldsymbol{z}_{P_i} + \boldsymbol{A}_1 \cdot \dot{\boldsymbol{z}}_{P_i} + \frac{\partial \boldsymbol{f}_1}{\partial P_i}$$

has to be solved to obtain the partials $\boldsymbol{z}_{P_i}(t) \doteq \frac{\partial \boldsymbol{r}_0}{\partial P_i}(t)$, e.g., by:

- Numerical integration for initial osculating elements
- Numerical quadrature for dynamic parameters
- Linear combinations for pseudo-stochastic parameters

Reduced-dynamic orbit representation

Position epochs (in GPS time)

Positions (km) & Velocities (dm/s) (Earth-fixed)

Clock corrections are not provided

```
*  2009 11  2  0  0  0.00000000
PL15   -391.718353   6623.836682     79.317661 999999.999999
VL15  13710.157683   1908.731015 -77015.601314 999999.999999
*  2009 11  2  0  0 10.00000000
PL15   -377.980705   6625.284690      2.298385 999999.999999
VL15  13764.602016    987.250587 -77021.193676 999999.999999
*  2009 11  2  0  0 20.00000000
PL15   -364.190222   6625.811136    -74.721213 999999.999999
VL15  13815.825127     65.631014 -77016.232293 999999.999999
*  2009 11  2  0  0 30.00000000
PL15   -350.350131   6625.415949   -151.730567 999999.999999
VL15  13863.820409   -855.995477 -77000.719734 999999.999999
*  2009 11  2  0  0 40.00000000
PL15   -336.463660   6624.099187   -228.719134 999999.999999
VL15  13908.581905  -1777.497047 -76974.660058 999999.999999
*  2009 11  2  0  0 50.00000000
PL15   -322.534047   6621.861041   -305.676371 999999.999999
VL15  13950.104280  -2698.741871 -76938.058807 999999.999999
*  2009 11  2  0  1  0.00000000
PL15   -308.564533   6618.701833   -382.591743 999999.999999
VL15  13988.382807  -3619.598277 -76890.923043 999999.999999
```

Excerpt of reduced-dynamic GOCE positions at begin of 2 Nov, 2009

GO_CONS_SST_PRD_2__20091101T235945_20091102T235944_0001

LEO sensor offsets

Phase center offsets $\delta \boldsymbol{r}_{leo,ant}$:

- are needed in the inertial or Earth-fixed frame and have to be transformed from the satellite frame using **attitude data** from the star-trackers
- consist of a frequency-independent **instrument offset**, e.g., defined by the center of the instrument‘s mounting plane (CMP) in the satellite frame
- consist of frequency-dependent **phase center offsets** (PCOs), e.g., defined wrt the center of the instrument‘s mounting plane in the antenna frame (ARF)
- consist of frequency-dependent **phase center variations** (PCVs) varying with the direction of the incoming signal, e.g., defined wrt the PCOs in the antenna frame

LEO sensor offsets

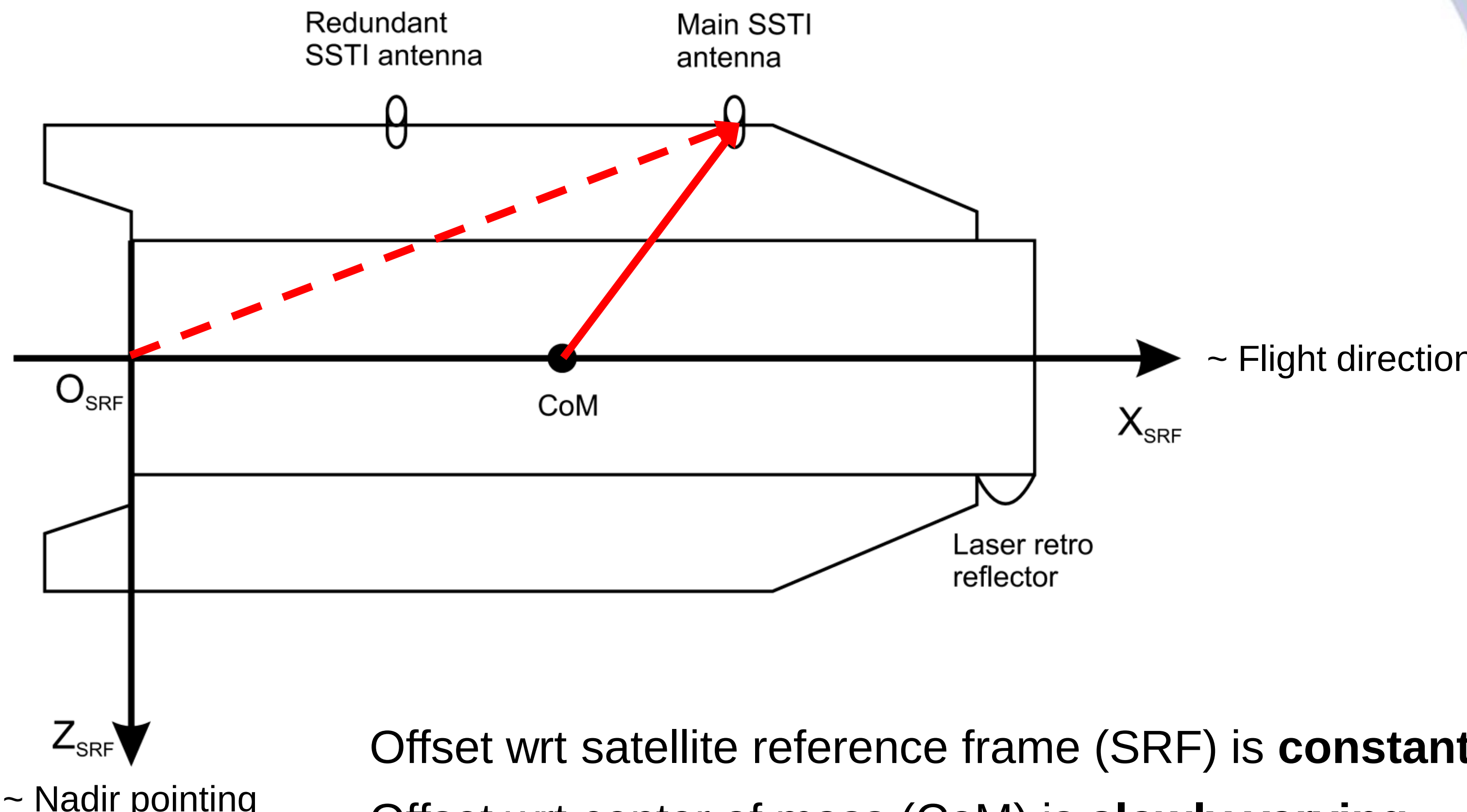

Offset wrt satellite reference frame (SRF) is **constant**

Offset wrt center of mass (CoM) is **slowly varying**

GOCE mission

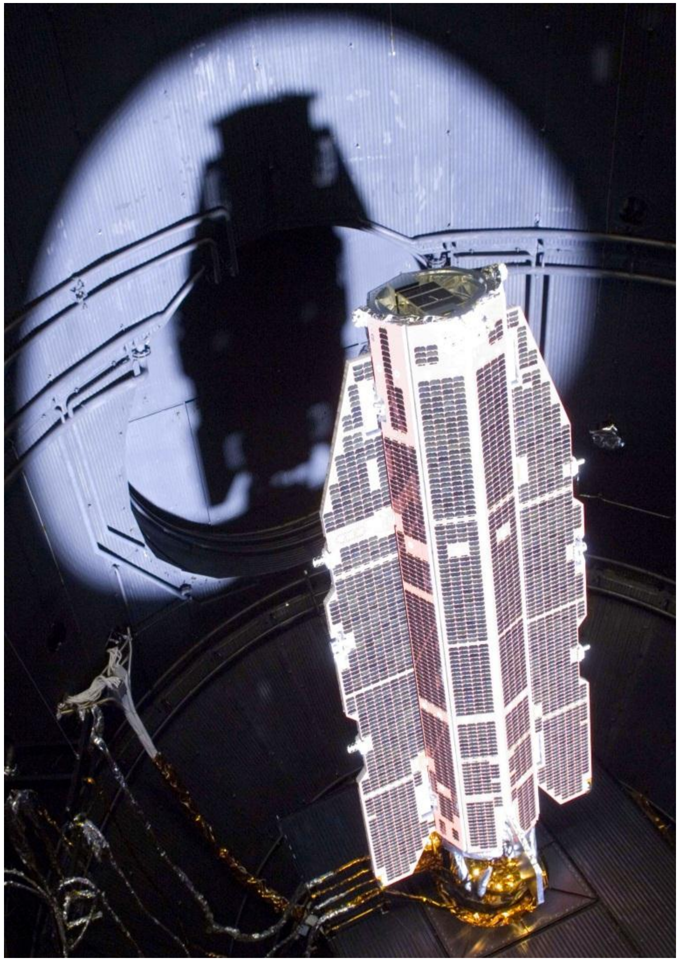

Courtesy: ESA

- **G**ravity and steady-state **O**cean **C**irculation **E**xplorer (**GOCE**)
- First Earth Explorer of the Living Planet Program of the European Space Agency
- Launch: 17 March 2009 from Plesetsk, Russia
- Sun-synchronous dusk-dawn orbit with an inclination of 96.6^o
- Altitude: 254.9 km
- Mass: 1050 kg at launch
- 5.3 m long, 1.1 m^2 cross section

GOCE orbit

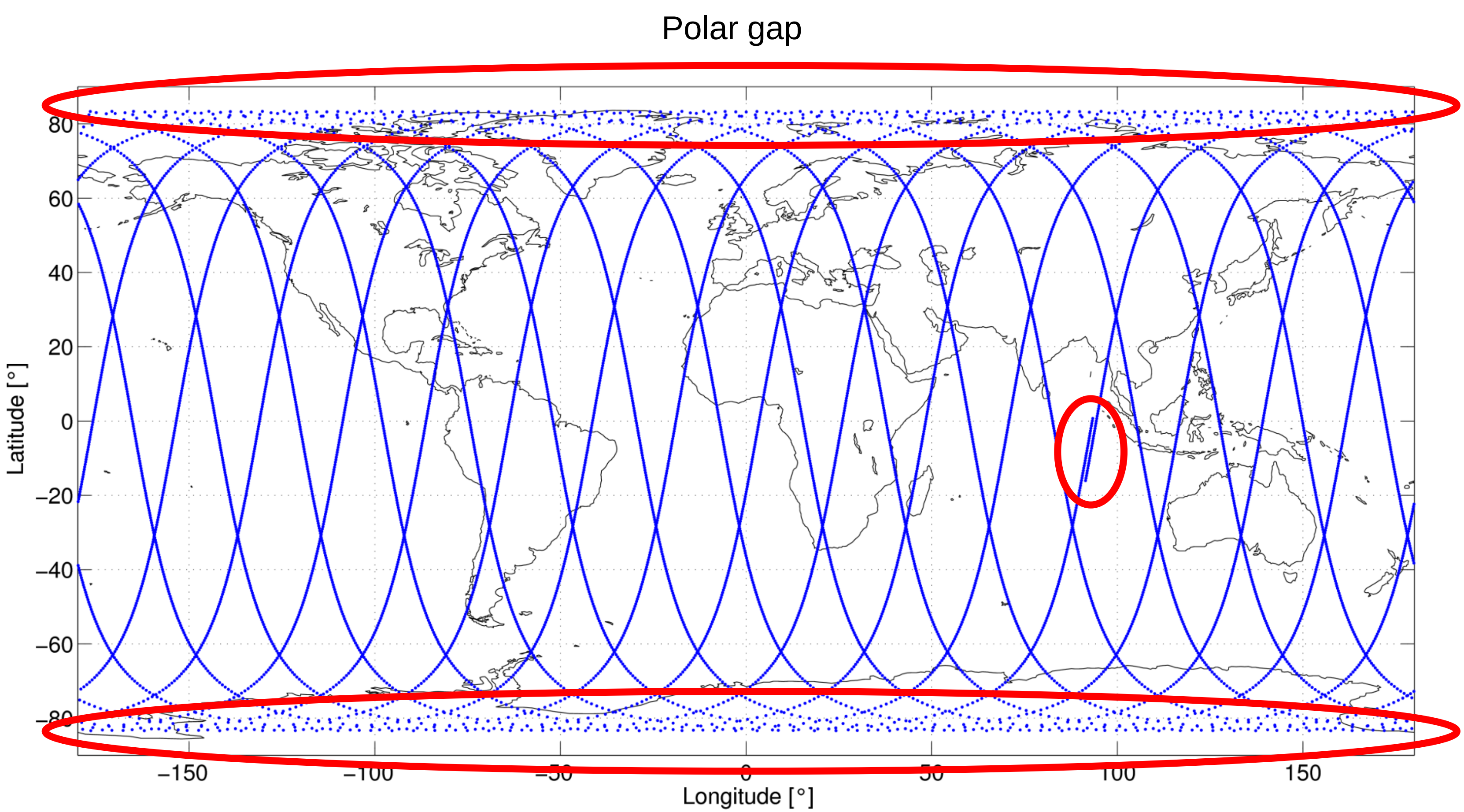

Ground-track coverage on 2 Nov, 2009

Complete geographical coverage after 979 revolutions (repeat-cycle of 61 days)

GOCE core instrument

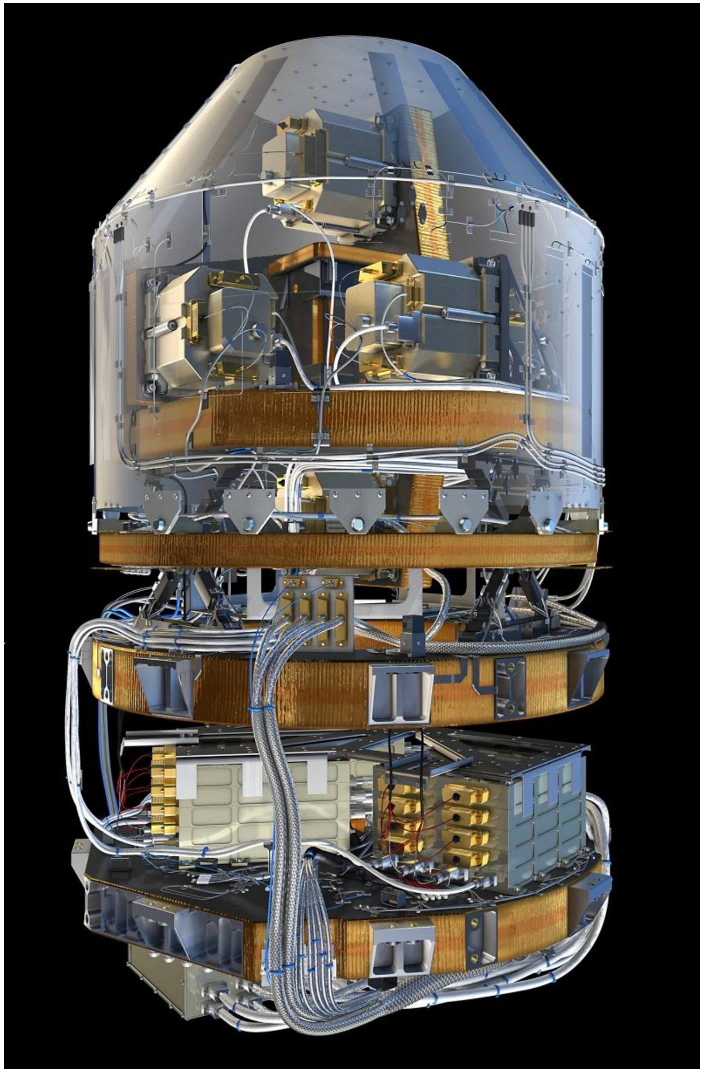

Courtesy: ESA

Core payload:

Electrostatic Gravity Gradiometer

three pairs of accelerometers

0.5 m arm length

Main mission goals:

Determination of the Earth's gravity field with an accuracy of 1mGal (= 10^{-5} m/s^2) at a spatial resolution of 100 km

Accelerometer noise:

ACC14: 3.9 10^{-12} m/s^2/Hz$^{1/2}$

ACC25: 3.1 10^{-12} m/s^2/Hz$^{1/2}$

ACC36: 6.7 10^{-12} m/s^2/Hz$^{1/2}$

GOCE attitude control

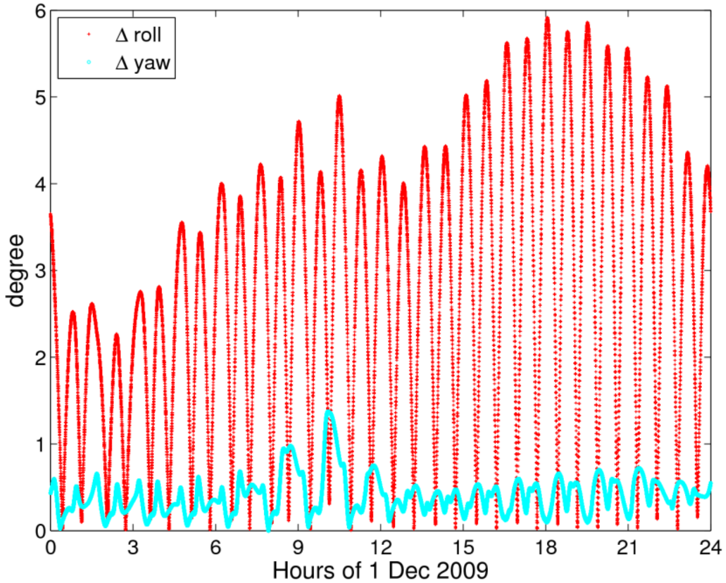

Courtesy: ESA

- Three axes stabilized, nadir pointing, aerodynamically shaped satellite
- Drag-free attitude control (DFAC) in flight direction employing a proportional Xe electric propulsion system
- Very rigid structure, no moving parts
- Attitude control by magnetorquers

- **Attitude measured by star cameras**
- **=> used for orbit determination**

GOCE SSTI

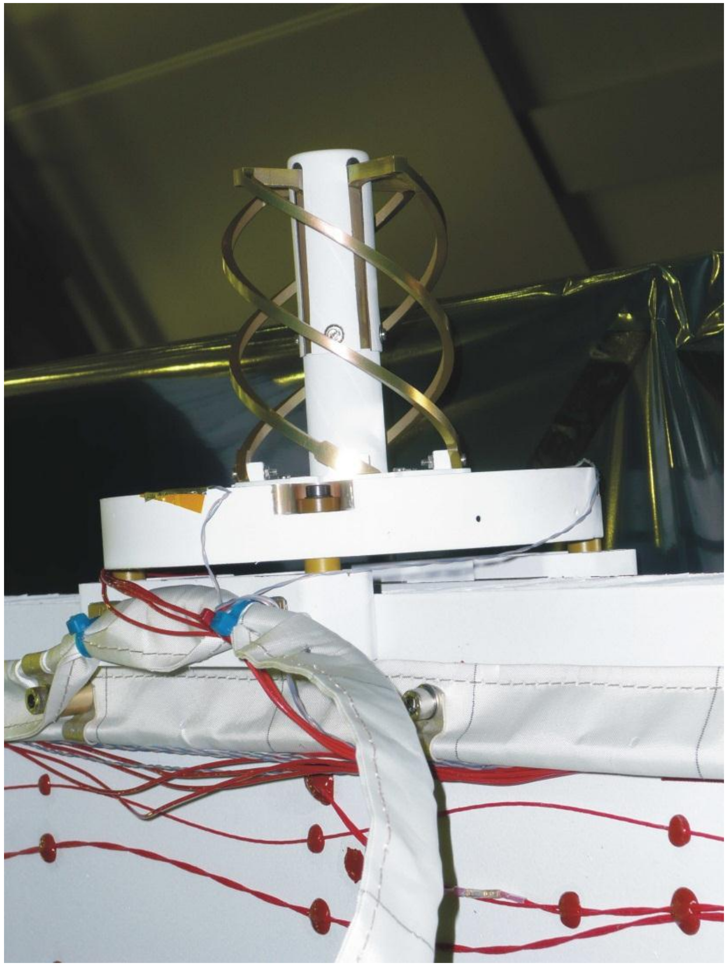

Courtesy: ESA

- **S**atellite-to-**S**atellite **T**racking **I**nstrument (**SSTI**)
- Dual-frequency L1, L2
- 12 channel GPS receiver
- Real time position and velocity (3D, 3 sigma < 100 m, < 0.3 m/s)
- 1 Hz data rate
- => Primary instrument for orbit determination

- **=> Mission requirement for precise science orbits: 2 cm (1D RMS)**

GOCE GPS antenna

L1, L2, Lc phase center offsets

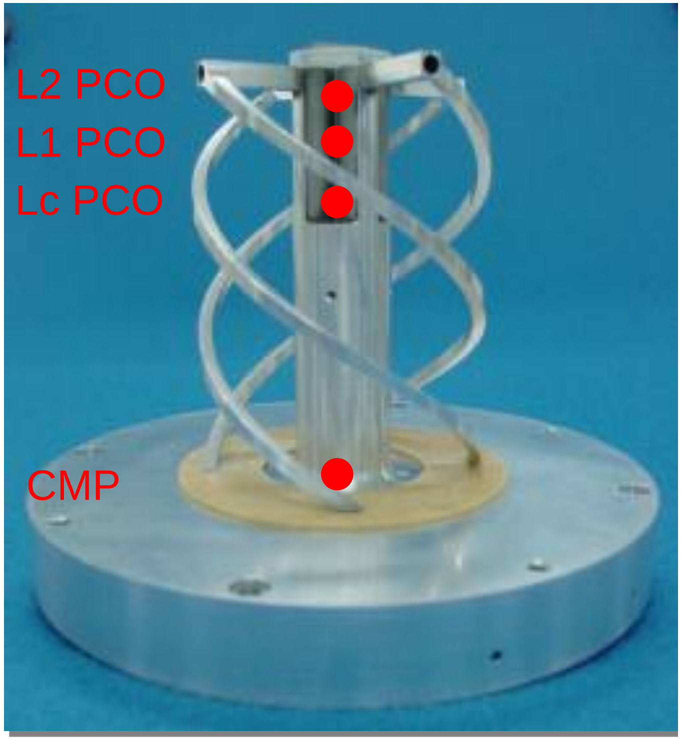

Measured from ground calibration
in anechoic chamber

Lc phase center variations

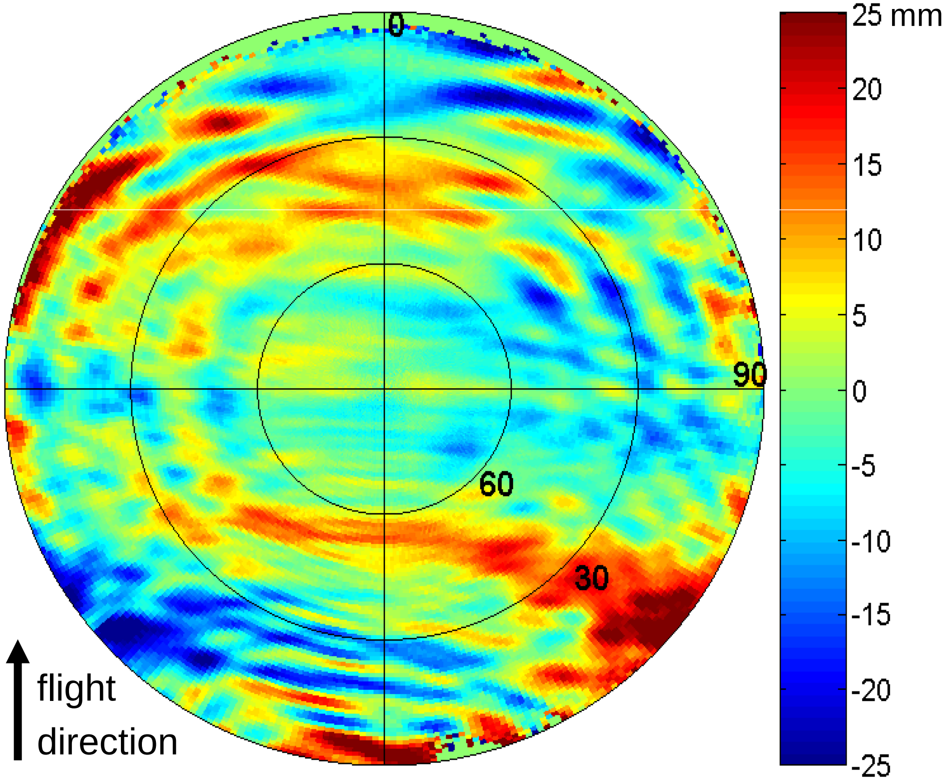

Empirically derived during orbit determination

GOCE High-level Processing Facility

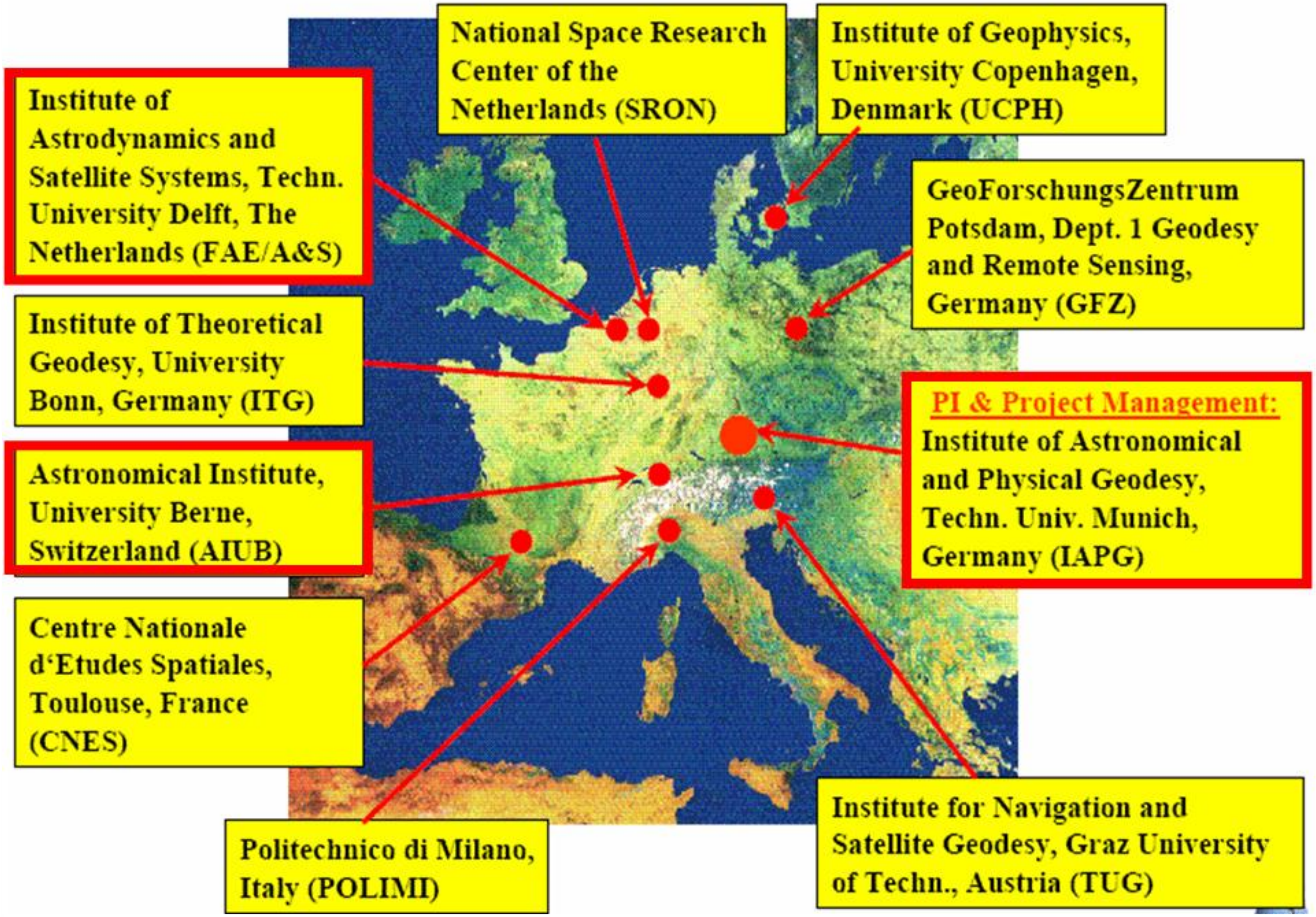

Responsibilities:

DEOS => **RSO**
(Rapid Science Orbit)

AIUB => **PSO**
(Precise Science Orbit)

IAPG => Validation

Co-rotating orbital frames

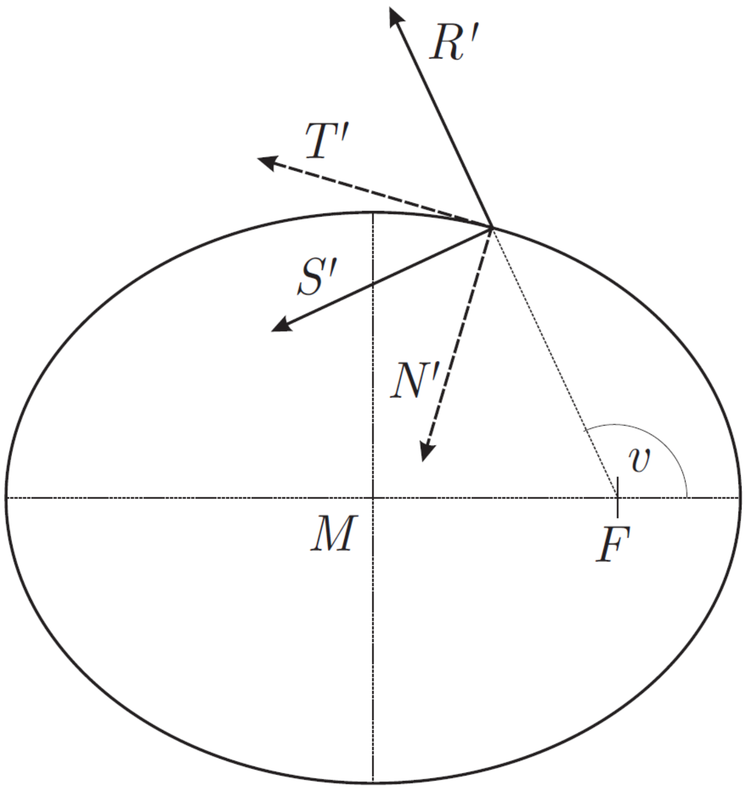

R', S', W' unit vectors are pointing:

- into the radial direction
- normal to **R'** in the orbital plane
- normal to the orbital plane (cross-track)

T', N', W' unit vectors are pointing:

- into the tangential (along-track) direction
- normal to **T'** in the orbital plane
- normal to the orbital plane (cross-track)

Small eccentricities: **S'**~**T'** (velocity direction)

Orbit differences KIN-RD

Differences at epochs of kin. positions

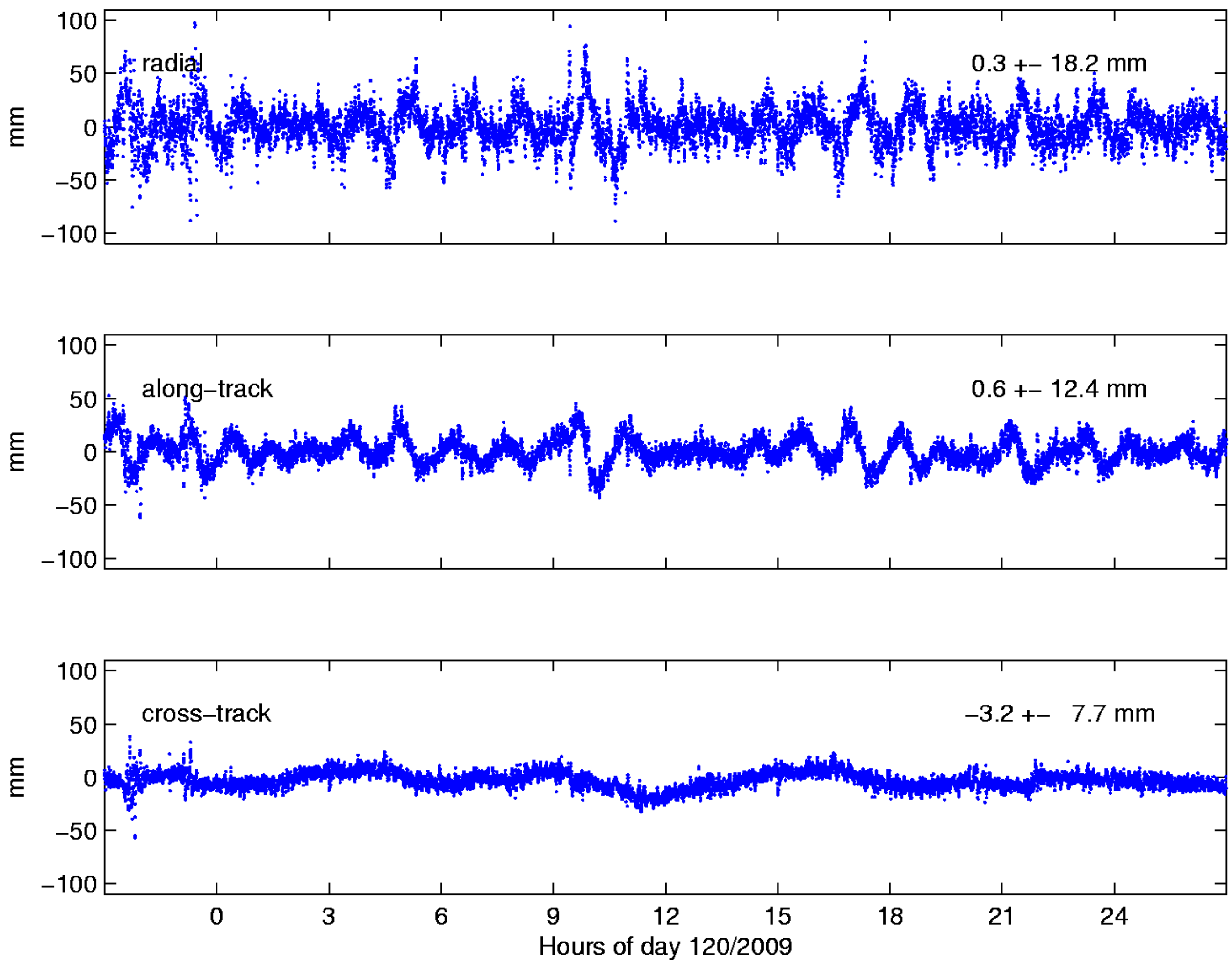

Orbit differences KIN-RD, time-differenced

Largest scatter of kin. positions

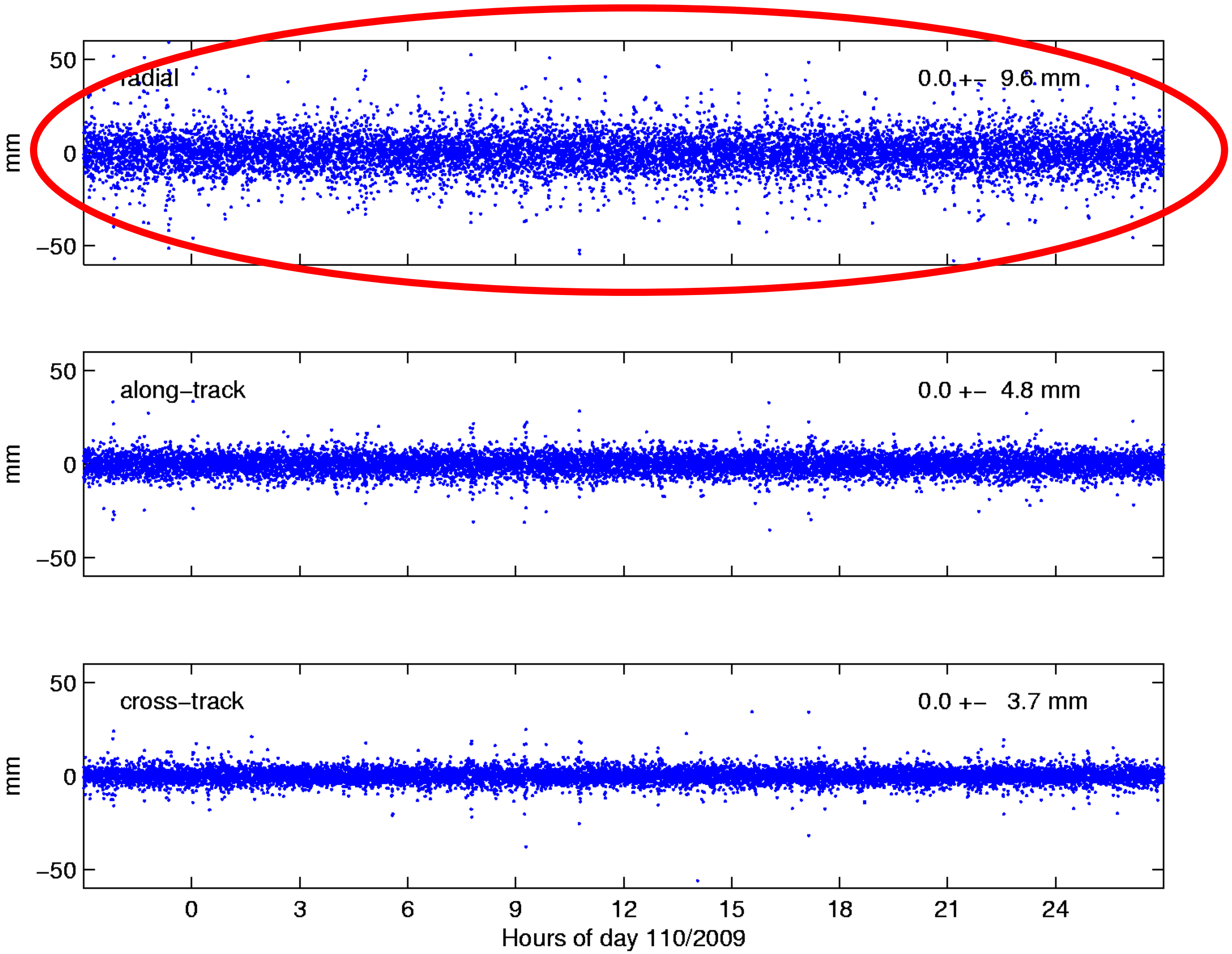

Pseudo-stochastic accelerations

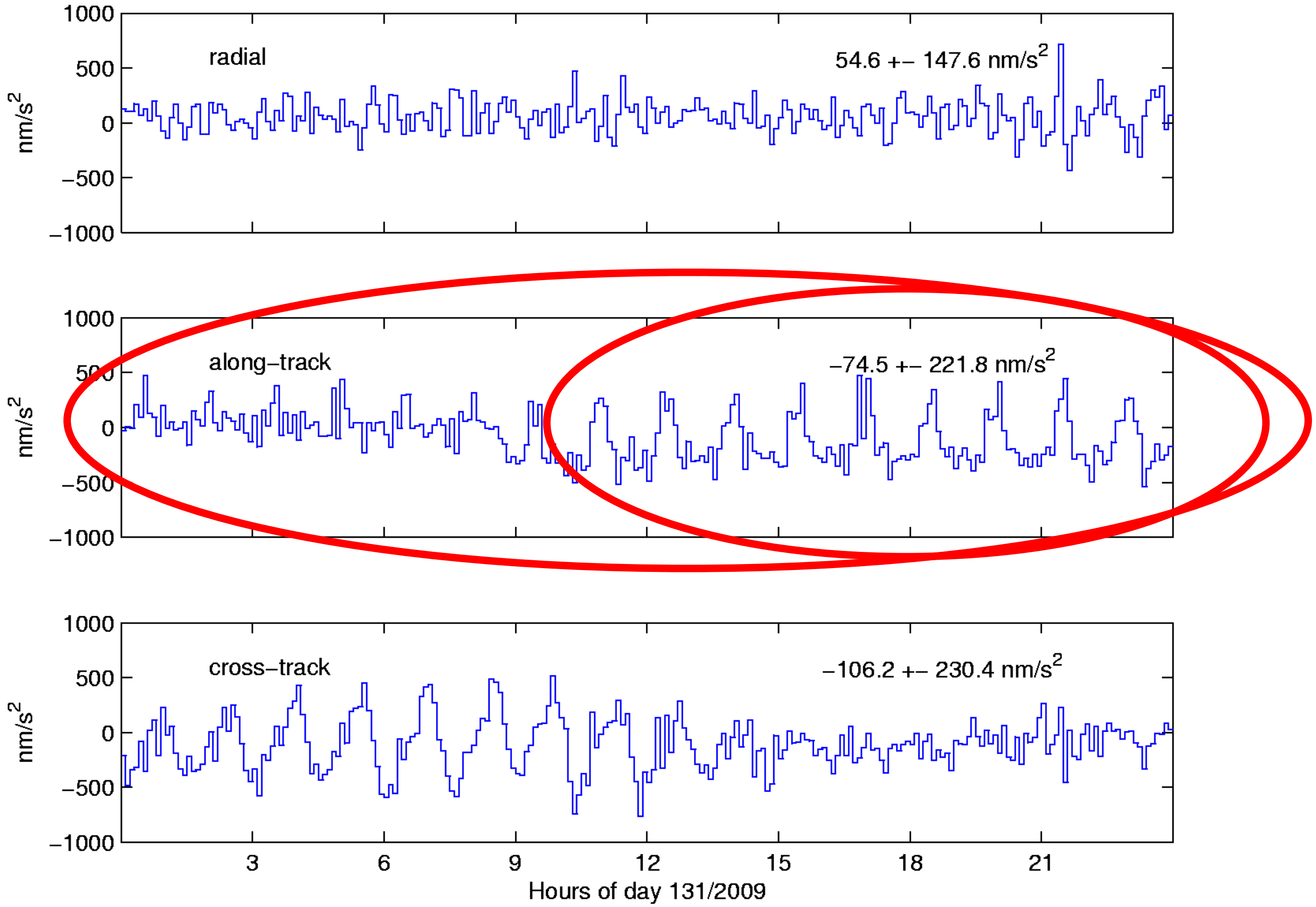

Largest signal due to air-drag

Eclipse-free flight on 17-May

Improving orbit determination

PCV modeling is one of the limiting factors for most precise LEO orbit determination. Unmodeled PCVs are systematic errors, which

- **directly** propagate into kinematic orbit determination and severly degrade the position estimates

- propagate into reduced-dynamic orbit determination to a smaller, **but still large extent**

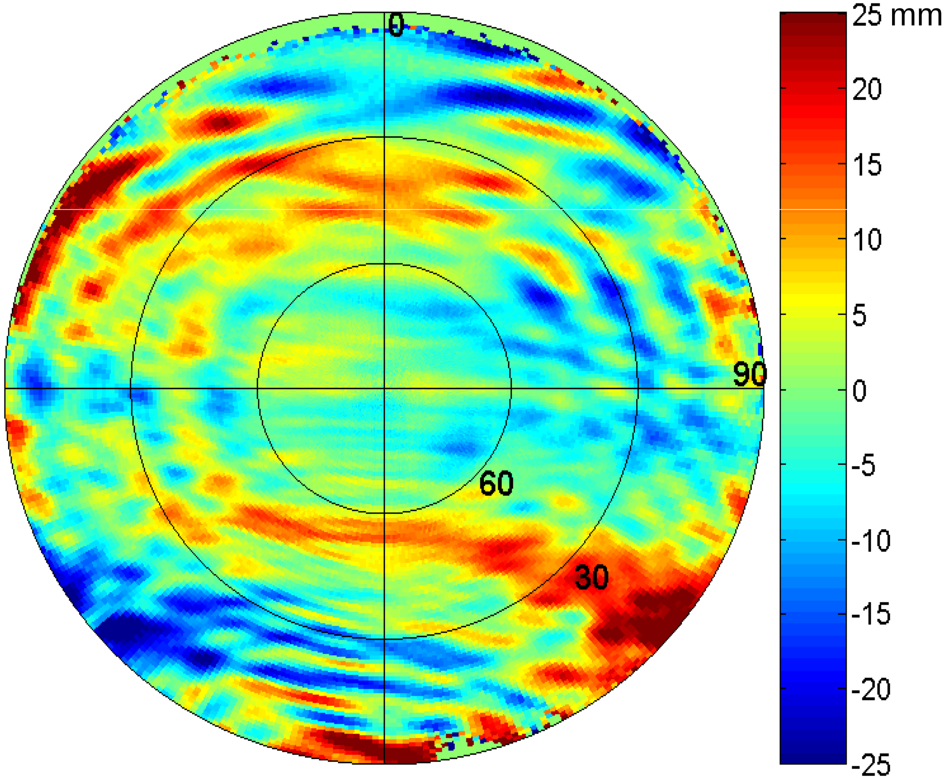

Improving orbit determination

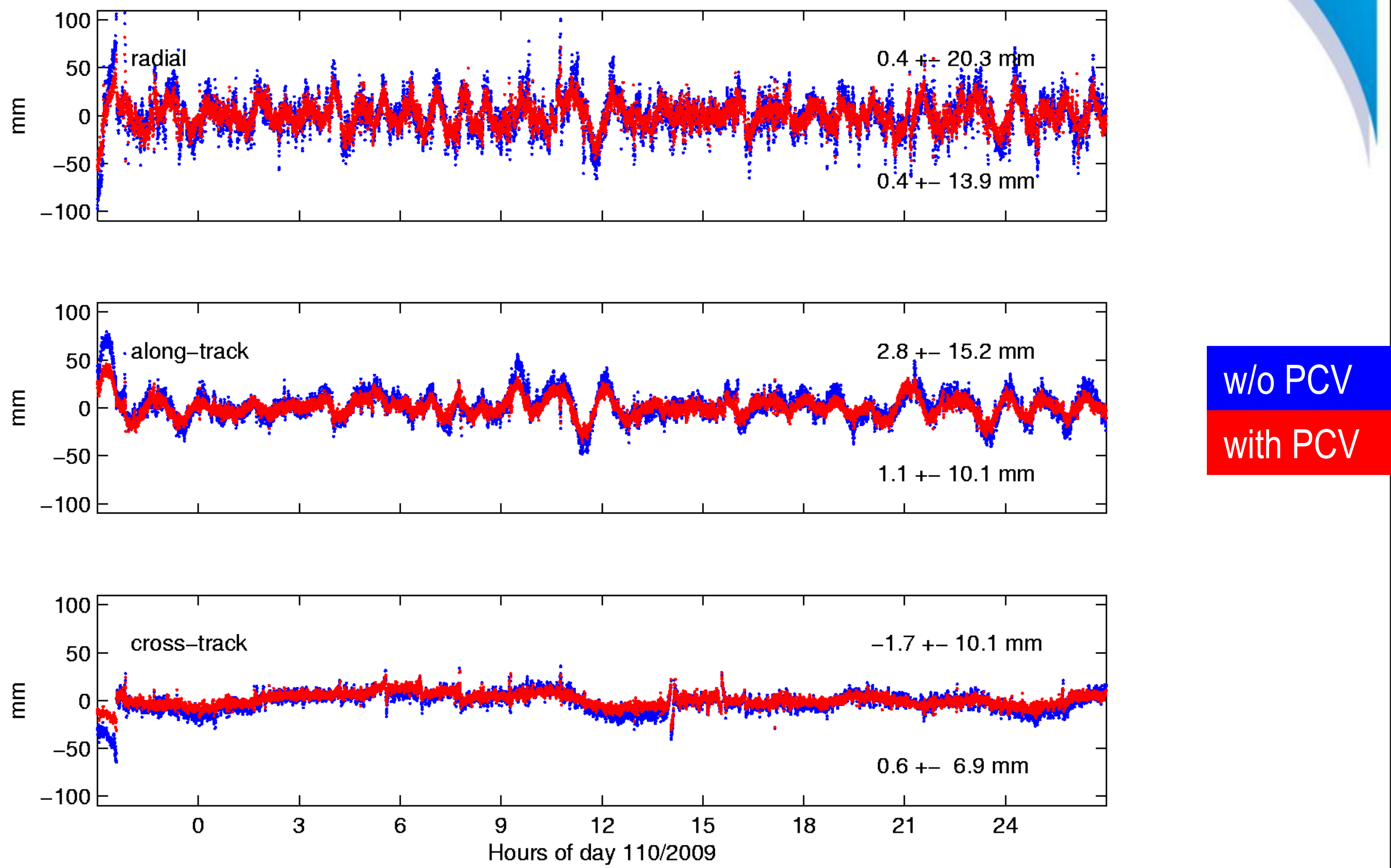

Orbit differences KIN-RD

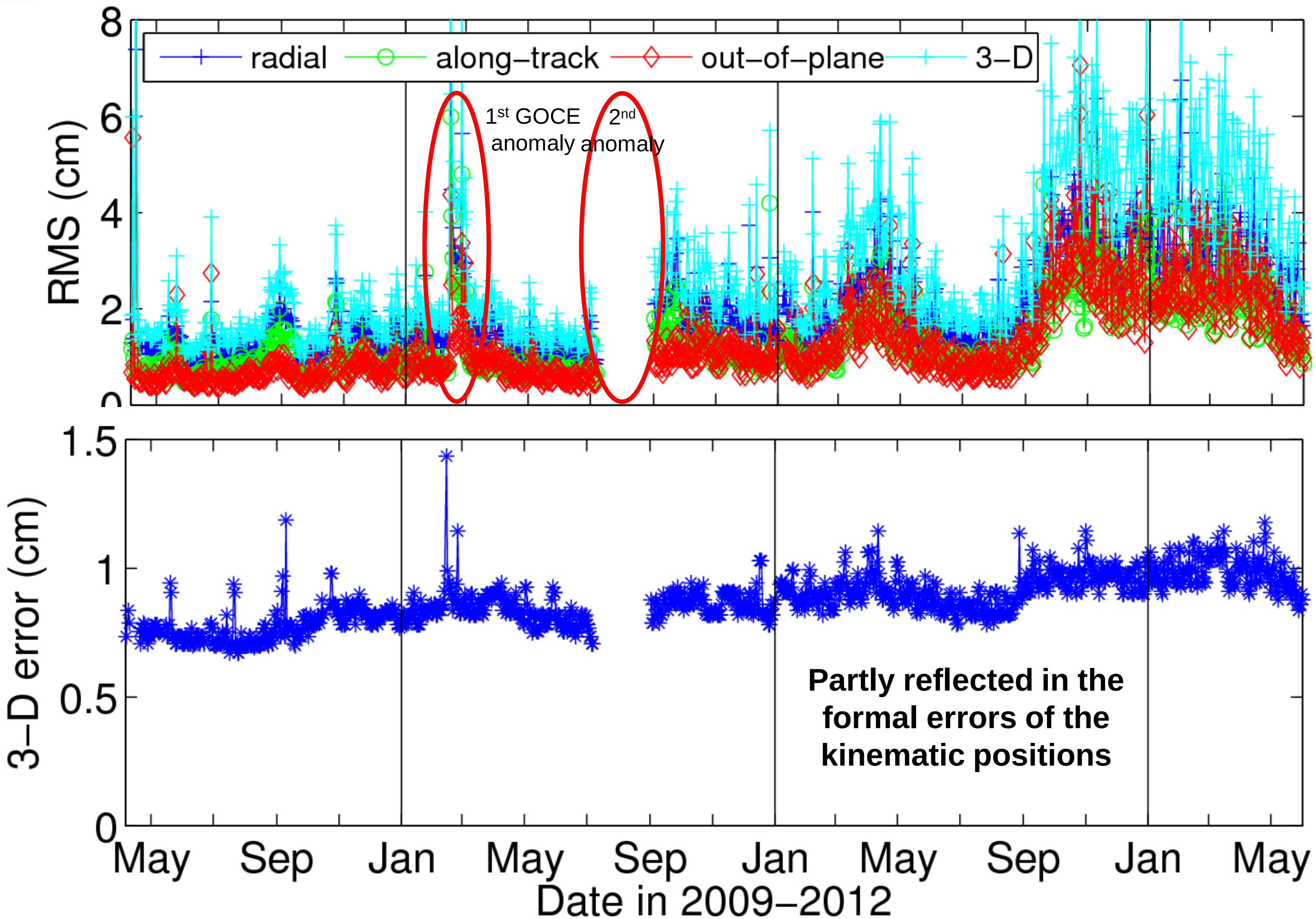

Orbit differences KIN-RD

Ascending arcs (RMS) | Descending arcs (RMS)

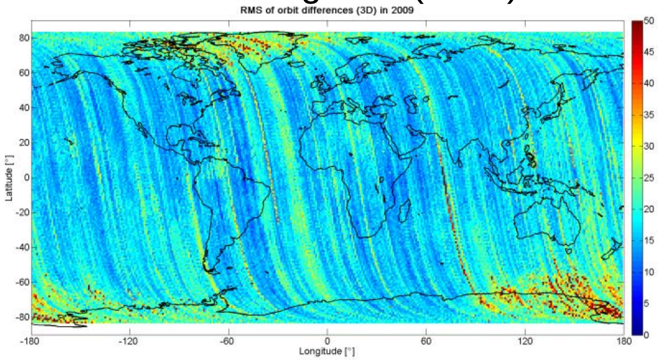

2009

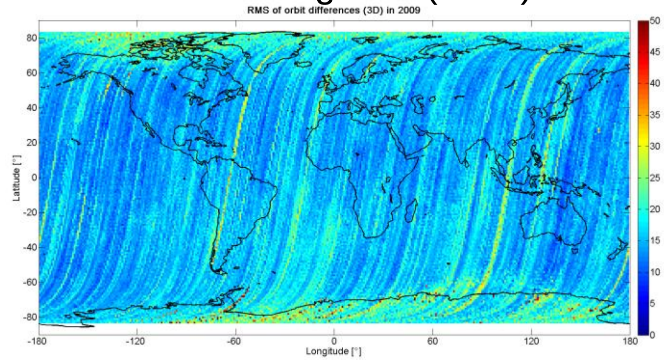

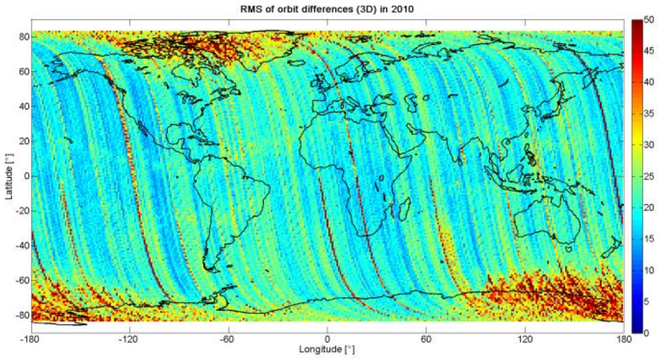

2010

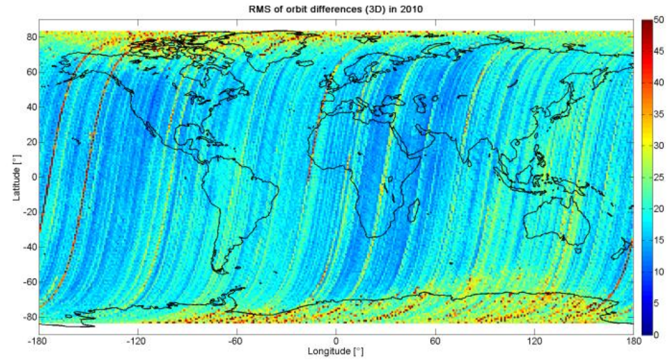

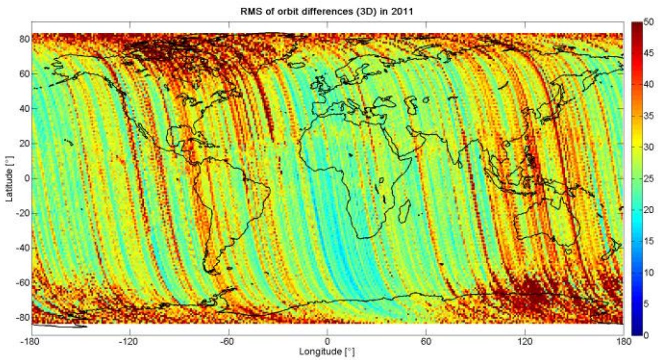

2011

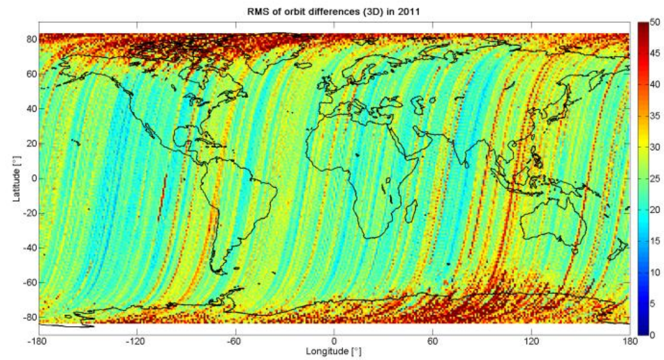

Orbit validation with SLR

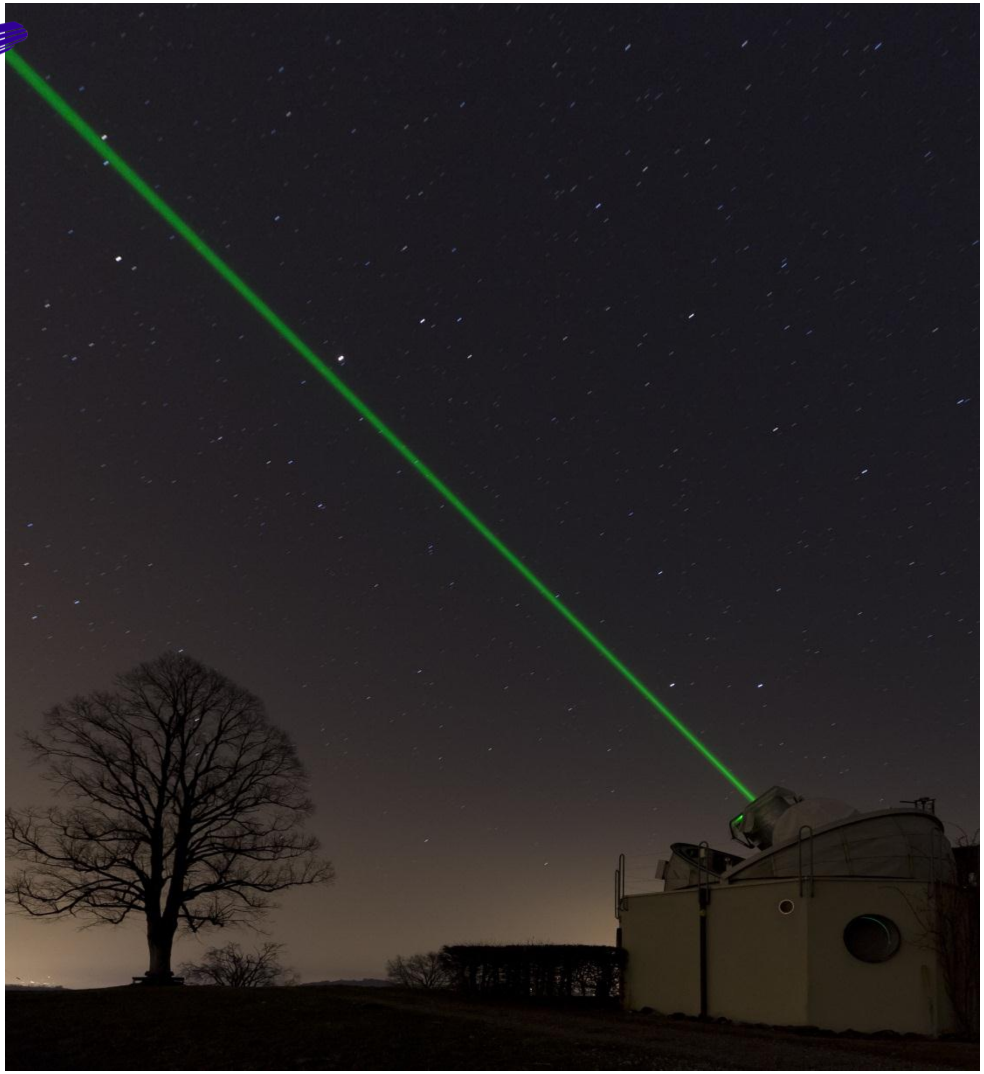

Zimmerwald SLR station

- 100 Hz Nd:YAG System
- 58 ps pulse length, 8 mJ energy
- Very autonomous operations
- Most productive station of the ILRS on the northern hemisphere

Example of an observed Lageos pass

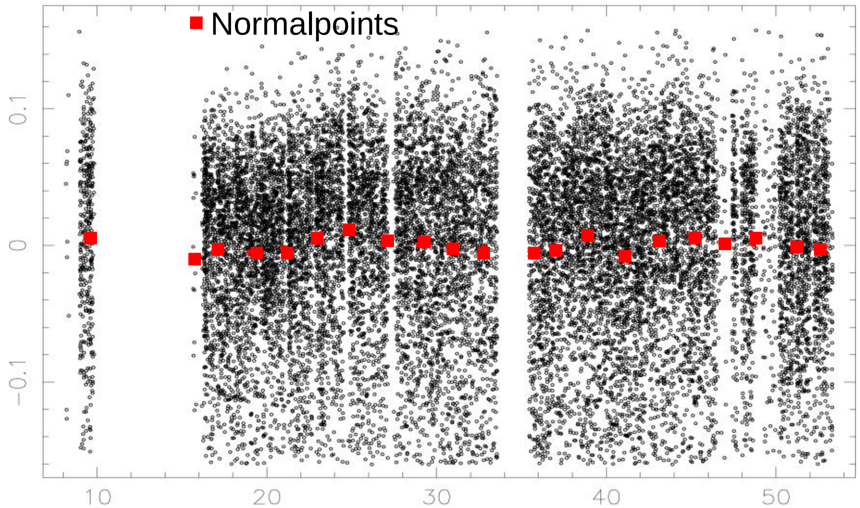

Orbit validation with SLR

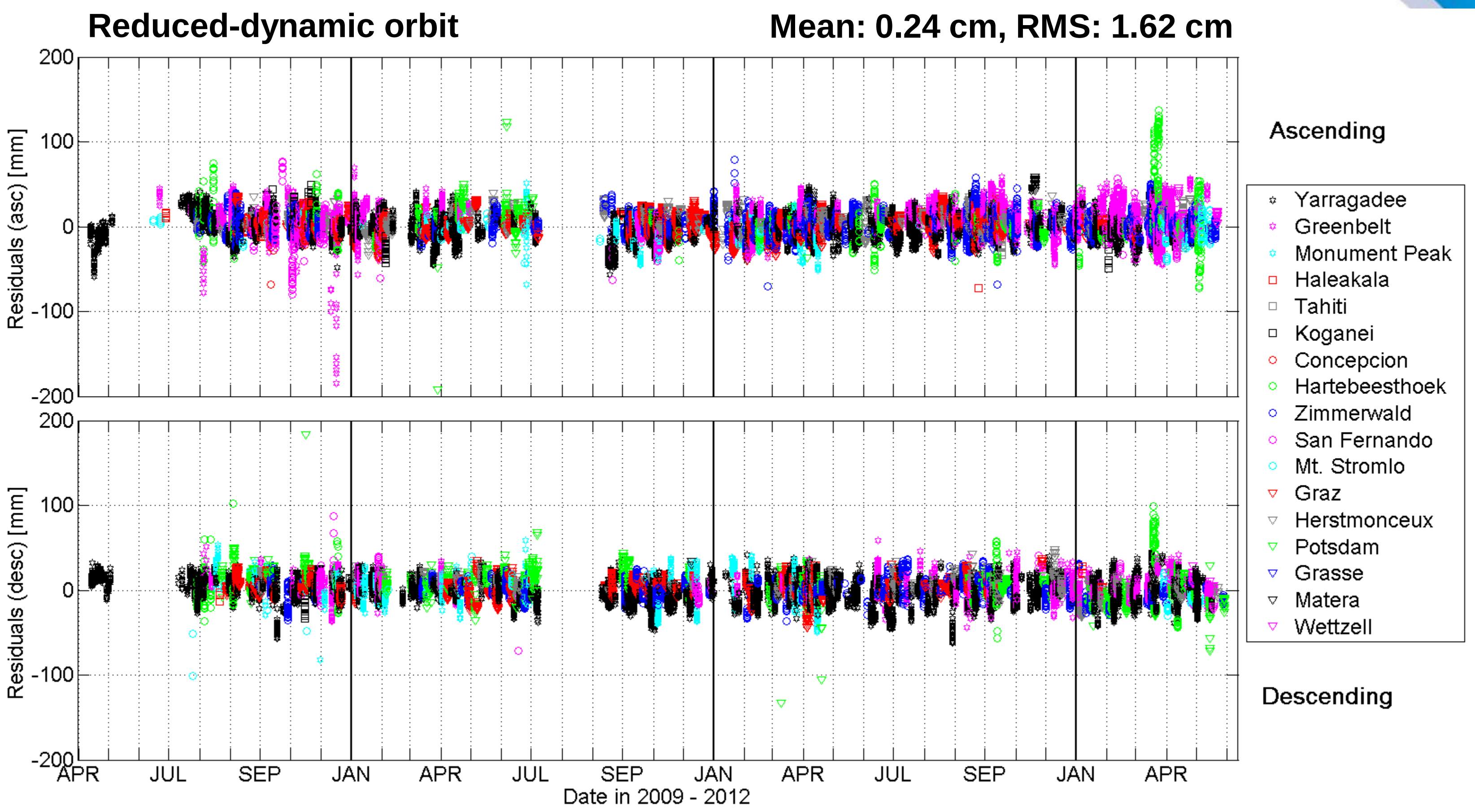

	2009:	2010:	2011:	2012:
RMS:	1.61 cm	1.44 cm	1.99 cm	2.05 cm
Mean:	0.46 cm	0.13 cm	0.25 cm	0.13 cm

Orbit validation with SLR

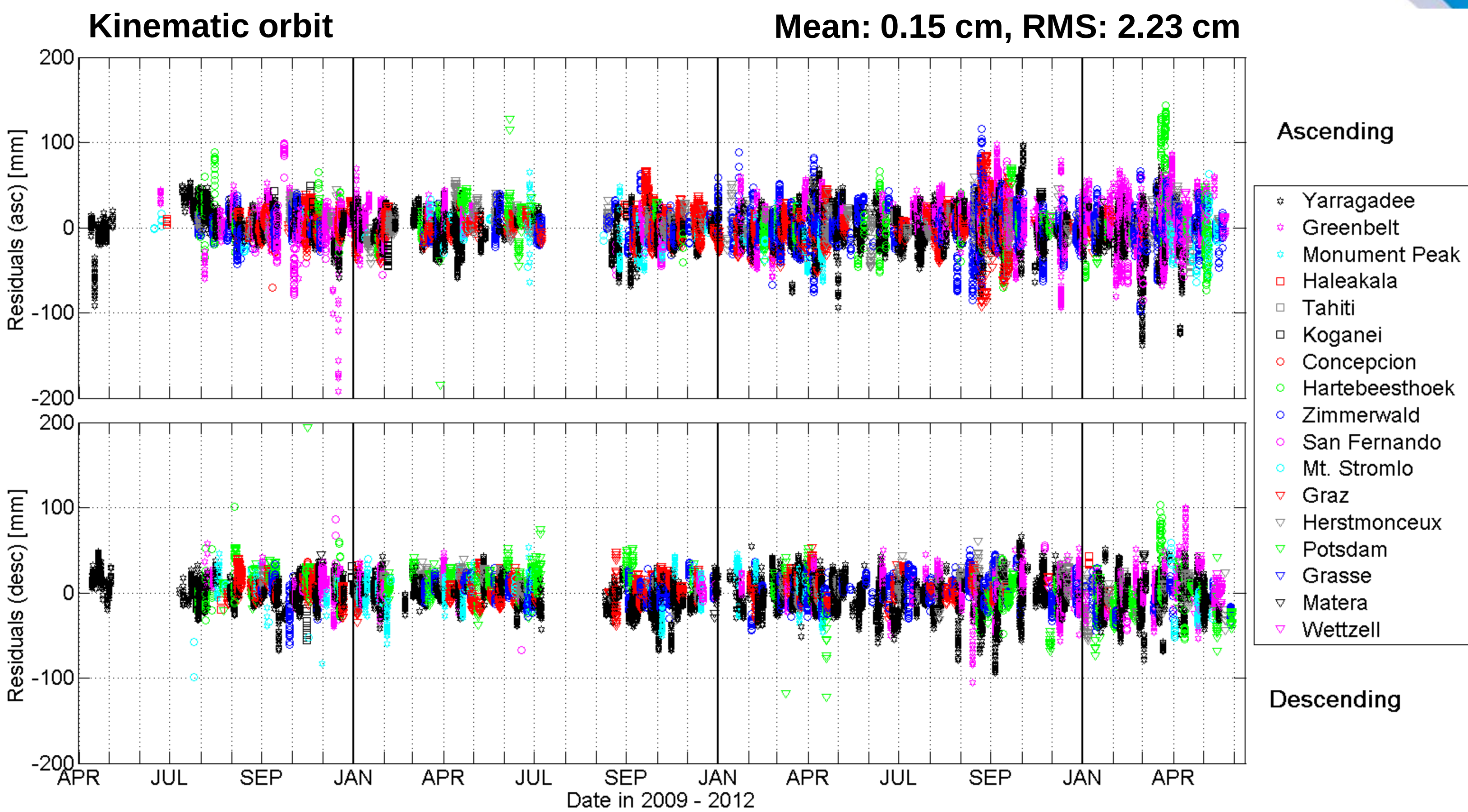

	2009:	2010:	2011:	2012:
RMS:	1.89 cm	1.76 cm	2.63 cm	3.00 cm
Mean:	0.49 cm	0.10 cm	0.15 cm	-0.24 cm

Improved SLR data modeling

- **use of SLRF2008 coordinate set**
- **application of azimuth- & nadir-dependent range corrections**

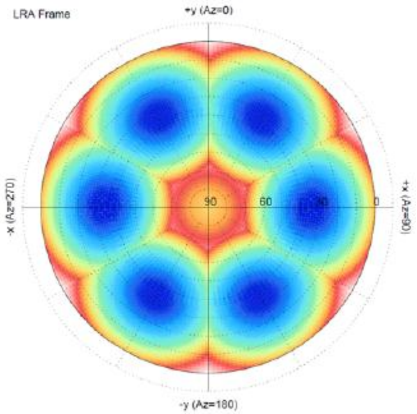

$$\Delta\rho_l = \left[L\sqrt{n_g^2 + (e^T n_l)^2 - 1}\right] - \left[e^T r_l\right]$$

Improved SLR data modeling

- **use of SLRF2008 coordinate set**
- **application of azimuth- & nadir-dependent range corrections**

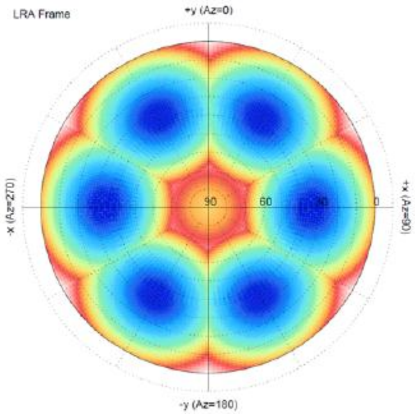

$$\Delta\rho_i = \left[L\sqrt{n_g^2 + (e^T n_i)^2 - 1}\right] - \left[e^T r_i\right]$$

(A): - SLRF2005 - no correction | **(B): - SLRF2008 - no correction** | **(C): - SLRF2008 - with correction**

SLR validation (cm) of red.-dyn. solutions (DOYs 251,2010 – 226,2011):

	Mean	**STD**
(A)	**0.37**	**1.62**
(B)	**0.52**	**1.45**
(C)	**0.01**	**1.44**

GOCE orbit parametrization

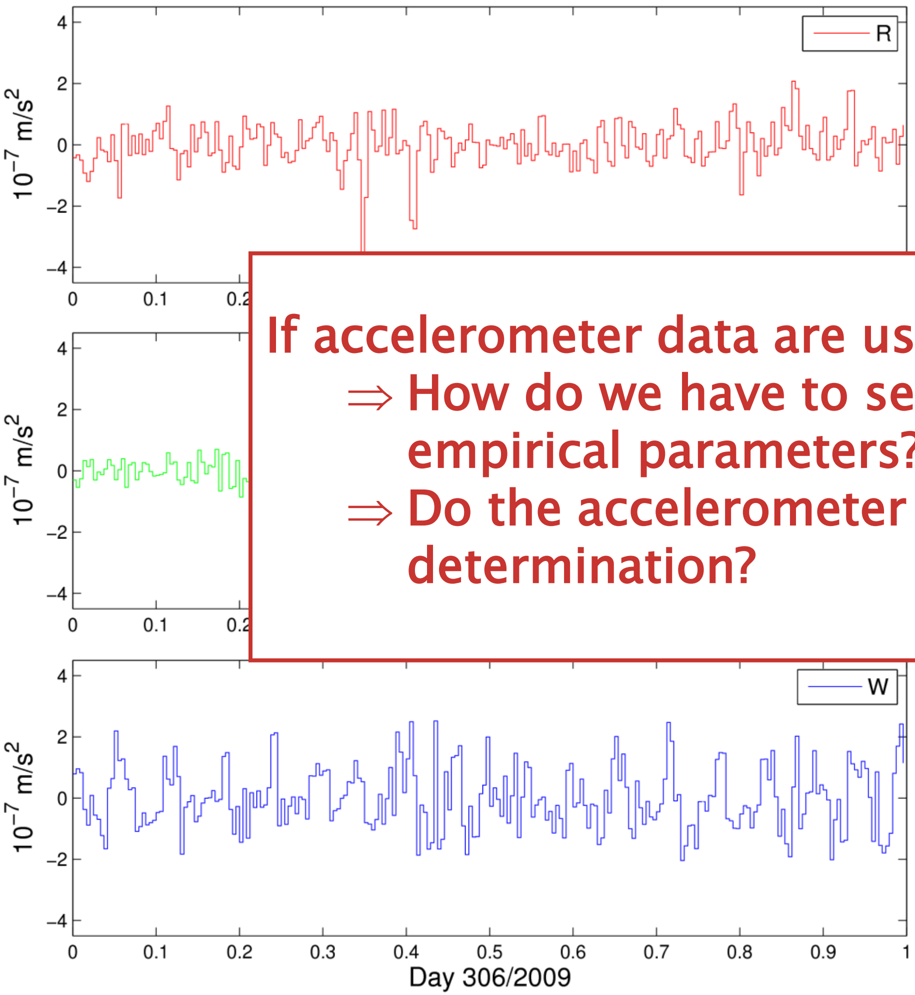

- Official **reduced-dynamic** solution is based on the following background models:
  - **Gravity field:** EIGEN5S (120x120)
  - 0x50)
  - al forces
  - six initial orbital elements
  - three constant accelerations in RSW
  - piece-wise constant accelerations (6 min) in RSW, constrained with σ=2.0*10^{-8} m/s^2

If accelerometer data are used for orbit determination:

⇒ How do we have to select the constraints for the empirical parameters?

⇒ Do the accelerometer data improve the orbit determination?

GOCE accelerometers

GRF: Gradiometer reference frame

X: flight direction

Z: nadir direction

Common mode accelerations provide a measure of the non-gravitational forces acting on the satellite

Common Mode:

$$a_{c,k,l,i} = \frac{1}{2}(a_{k,i} + a_{l,i})$$

Schematic view of GOCE gradiometer

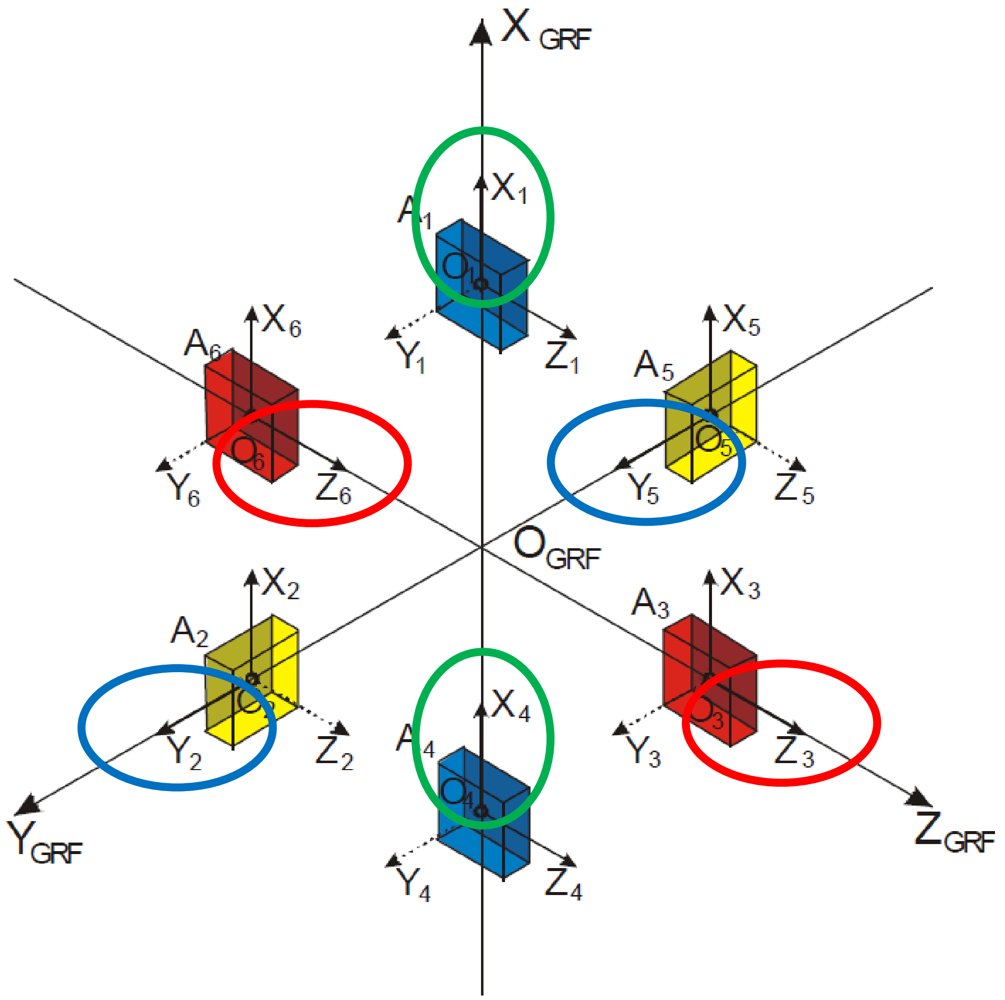

Common-mode accelerometer data

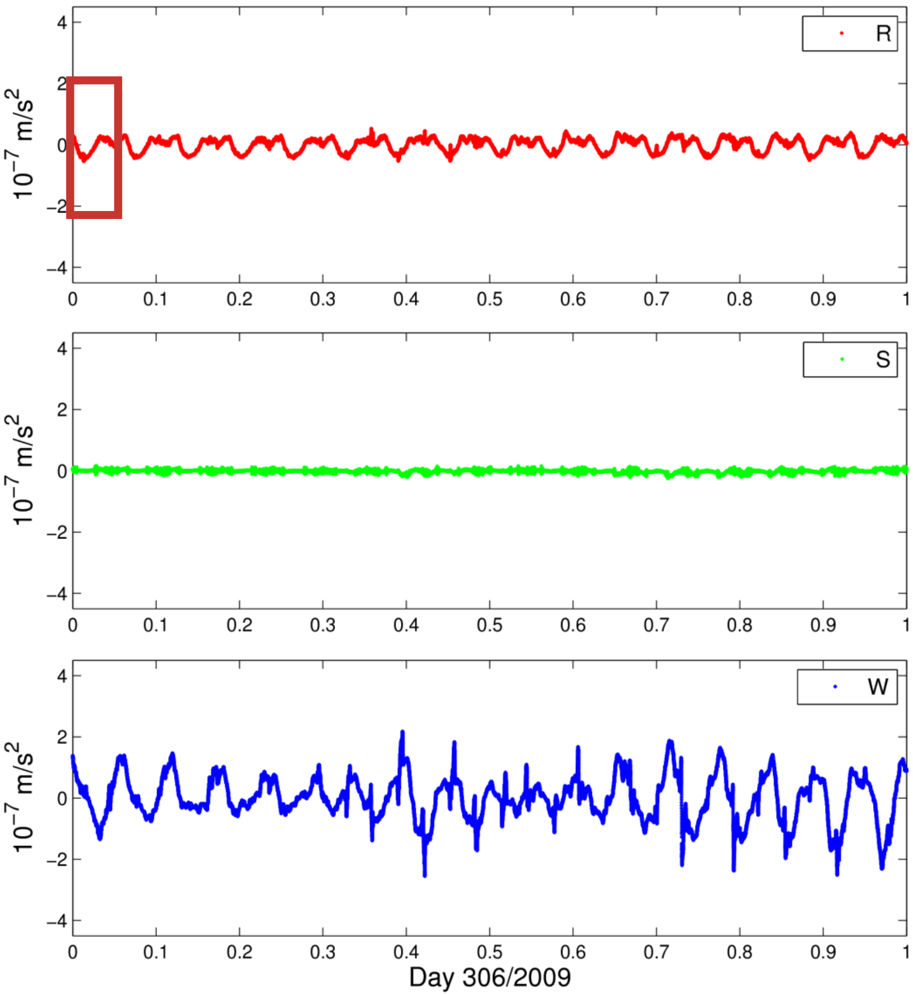

Meann offset removed, data transformed from XYZ into RSW directions

- **R** shows variations proportional to the thruster pulses (~3% cross-coupling)
- **S** is very small due to atmospheric drag compensation (drag-free flight)
- **W** shows largest variations due to the attitude motion (up to 5 degrees)
  - atmospheric drag acting on the satellite visible in W

Common-mode accelerometer data

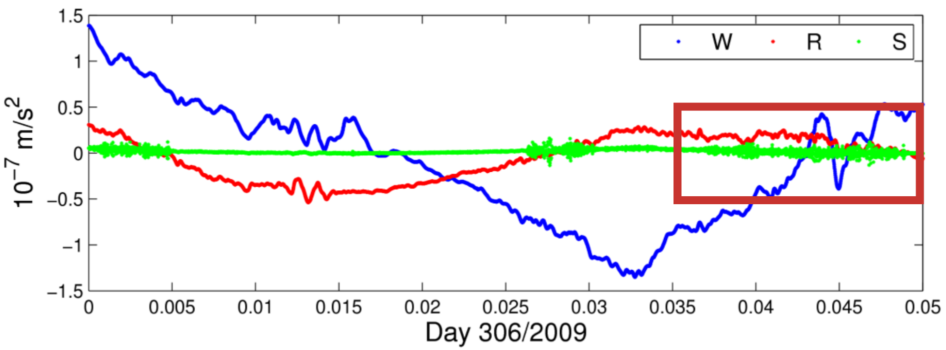

- Very clean data, no outliers

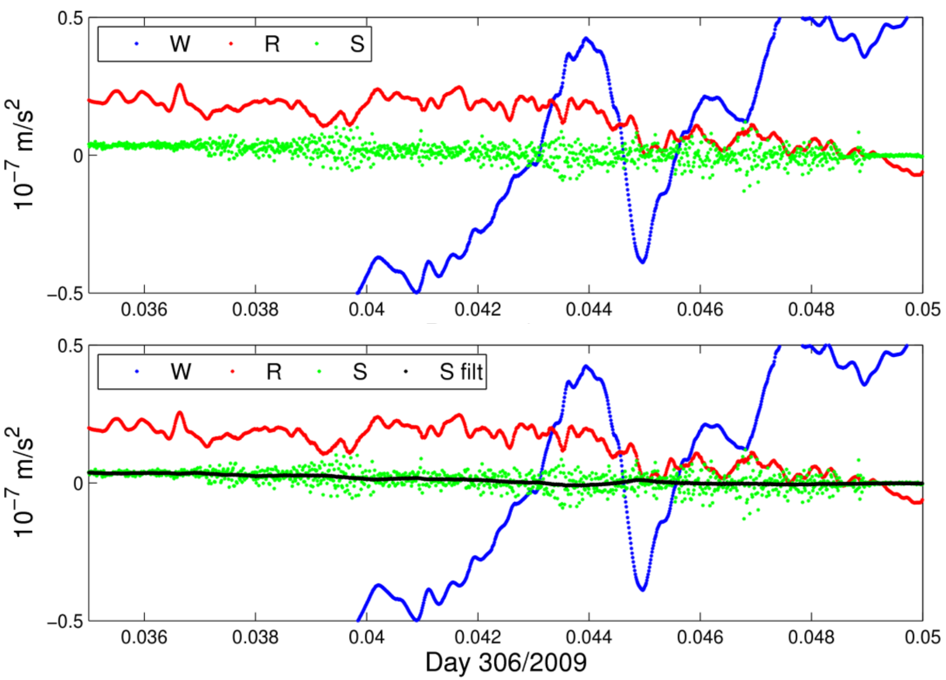

- Only S-component shows some noisy parts
- S-component may be filtered

Common-mode accelerometer data

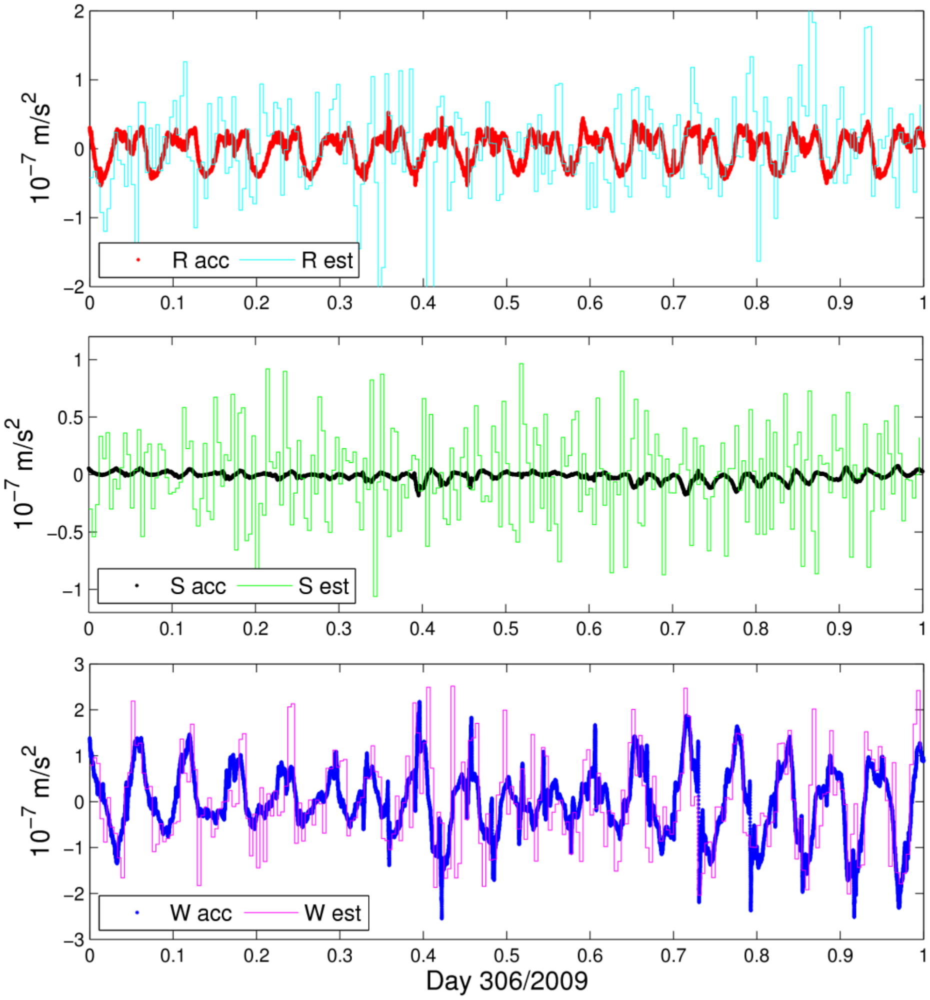

Note the different scaling of the plots

- Comparison of accelerometer data with estimated piece-wise constant accelerations shows
  - small correlation for R
  - no correlation for S
  - high correlation for W
- How do we have to select the constraints for the empirical parameters?
- Do the accelerometer data improve the orbit determination?

Reference solution

- Data set: DOYs 306-364, 2009
- **Solution A0 =>** reference orbits: GOCE “official” reduced-dynamic orbit solution, 24h instead of 30h batches
  - EIGEN5S (120x120), FES2004 (50x50)
  - Six initial orbital elements
  - Three constant accelerations over 24h in RSW
  - Piece-wise (6-min) constant accelerations in RSW $\sigma = 2.0*10^{-8}$ m/s^2
- SLR validation: **Mean 0.35 cm**, **RMS 2.01 cm**

Alternative solutions

Different models:

- **A**: EIGEN5S (120x120), FES2004 (50x50)
  w/o accelerometer data
- **B**: EIGEN5S (120x120), FES2004 (50x50) with acc
- **C**: GOCO03S (120x120), EOT08A (50x50) with acc
- **D**: GOCO03S (160x160), EOT08A (50x50) with acc

Different constraints:

- **0**: $\sigma_R = \sigma_S = \sigma_W = 2.0*10^{-8}$ m/s^2
- **1**: $\sigma_R = \sigma_S = \sigma_W = 5.0*10^{-9}$ m/s^2
- **2**: with acc $\sigma_R = 2.0*10^{-9}$ m/s^2 w/o acc: $2.0*10^{-8}$ m/s^2
  with acc $\sigma_S = 4.0*10^{-10}$ m/s^2 w/o acc: $4.0*10^{-9}$ m/s^2
  with acc $\sigma_W = 7.0*10^{-9}$ m/s^2 w/o acc: $7.0*10^{-8}$ m/s^2

What are reasonable constraints?

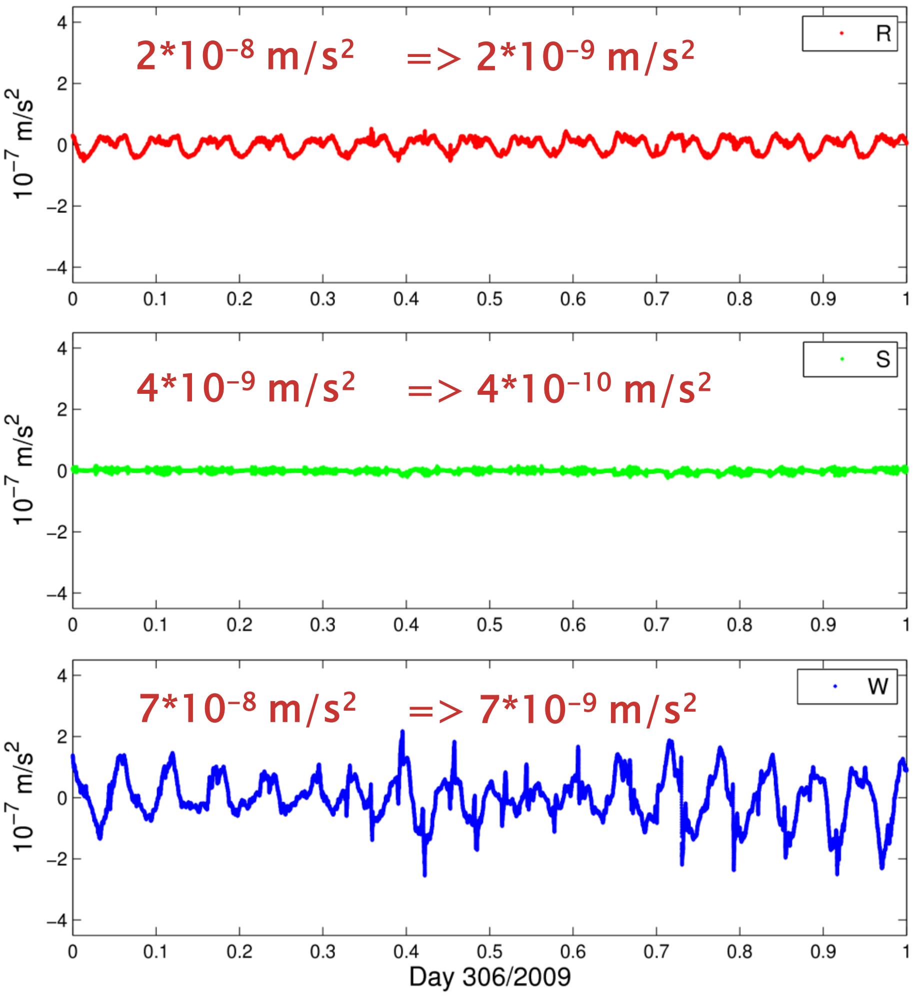

- The variations of the accelerations differ very much in **R**, **S**, **W**
- Use of different constraints for the three directions is thus reasonable
- Constraints, if **no** accelerometer data are used, are derived from:
  - Mean values for 6-min bins
  - RMS of these mean values => stable for the 57 days
- Constraints, if accelerometer data **are** used:
  - 10% - assuming that background models are sufficient

Comparison of estimated accelerations

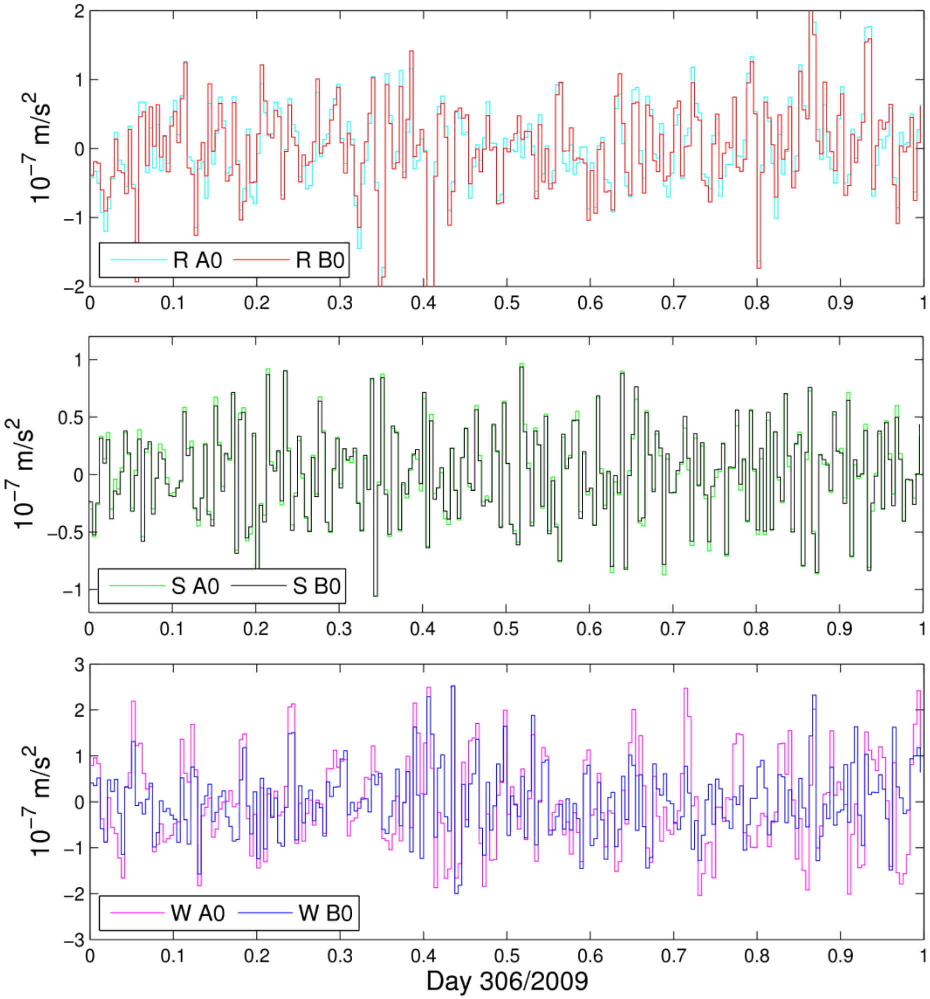

Note the different scaling of the plots

- **Comparison A0 ⇔ B0**
  - Difference: use of accelerometer data for B0
- **R**, **S**: no/small reduction of amplitude of empirical parameters
- **W**: some reduction is visible

=> Use of accelerometer data with the same parametrization in R,S,W has only impact on estimated accelerations in W

Comparison of estimated accelerations

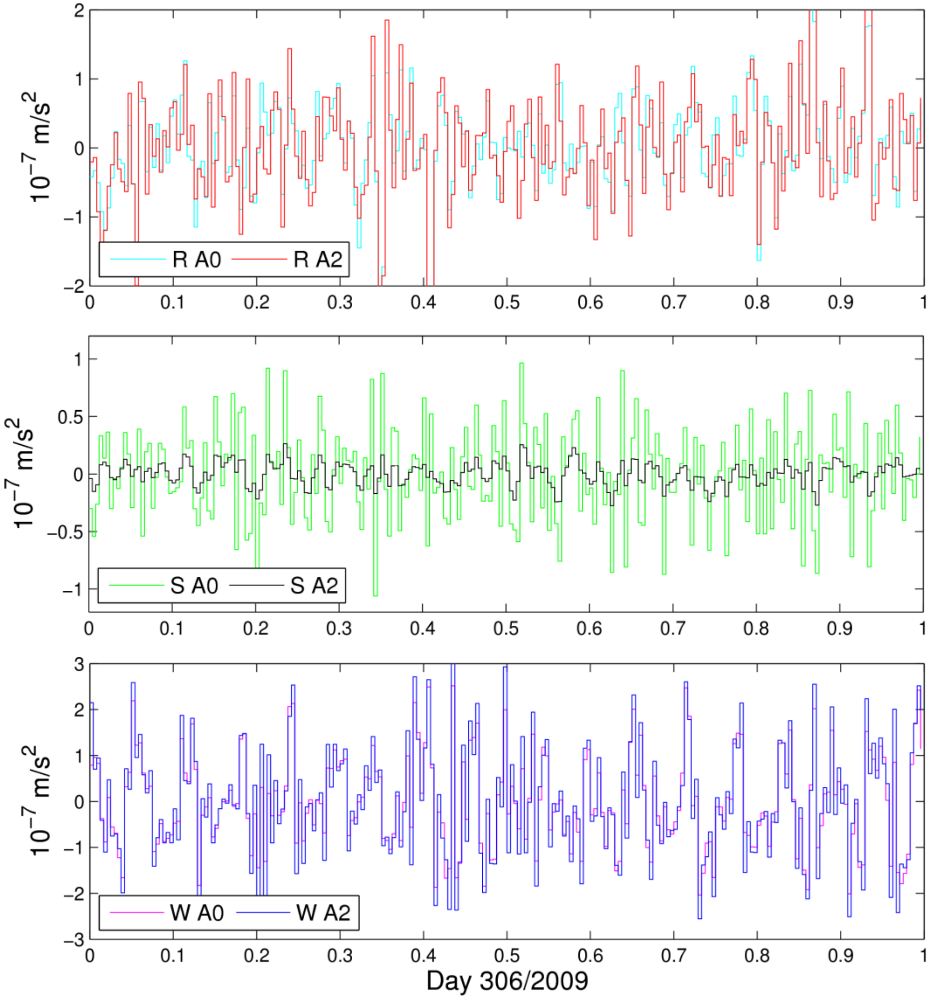

Note the different scaling of the plots

- **Comparison A0 ⇔ A2**
  - Difference: realistic constraints for A2
- **R**: few differences
- **S**: high reduction of amplitude
- **W**: slight increase of amplitude

=> Use of realistic constraints has impact on the amplitude of the accelerations related to looser or tighter constraints

Comparison of estimated accelerations

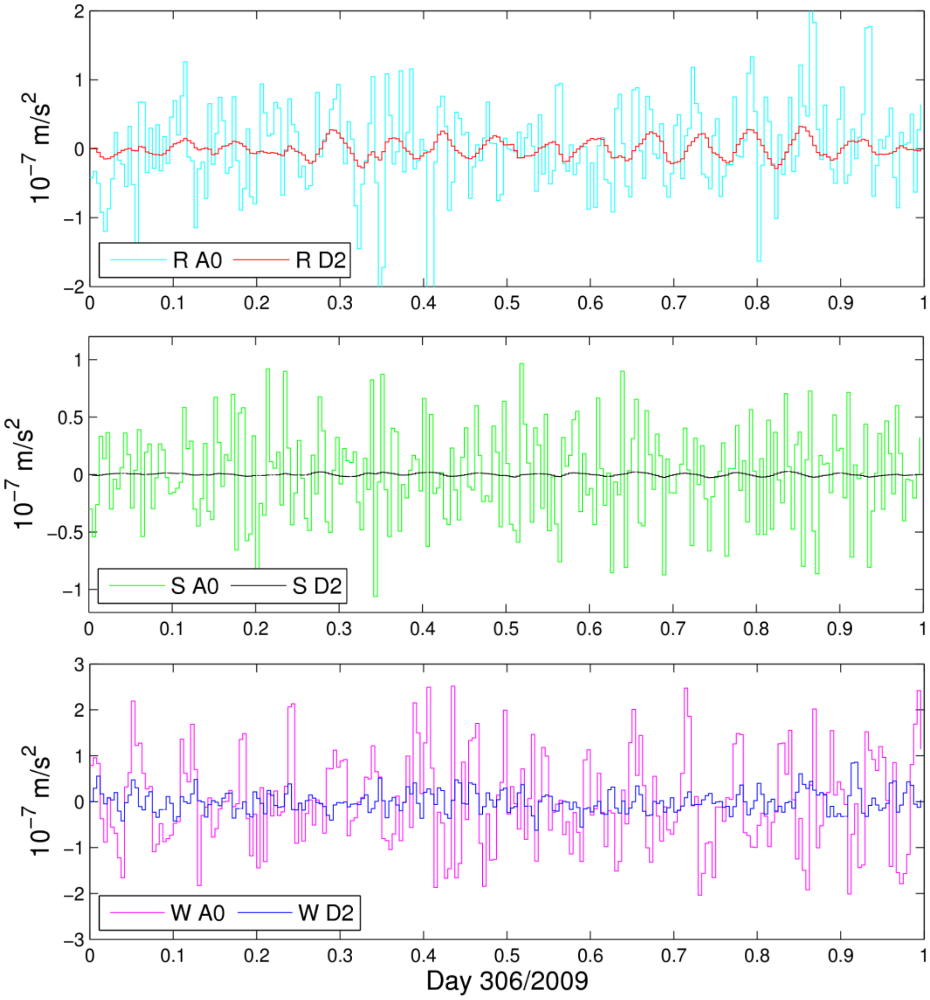

Note the different scaling of the plots

- **Comparison A0 ⇔ D2**
  - Difference: use of accelerometer data + "best possible" background models + realistic constraints (10%)
- **High** reduction for all components

=> Use of accelerometer data + realistic constraints has impact on the amplitude of the accelerations related to tighter constraints

Validation of orbit quality

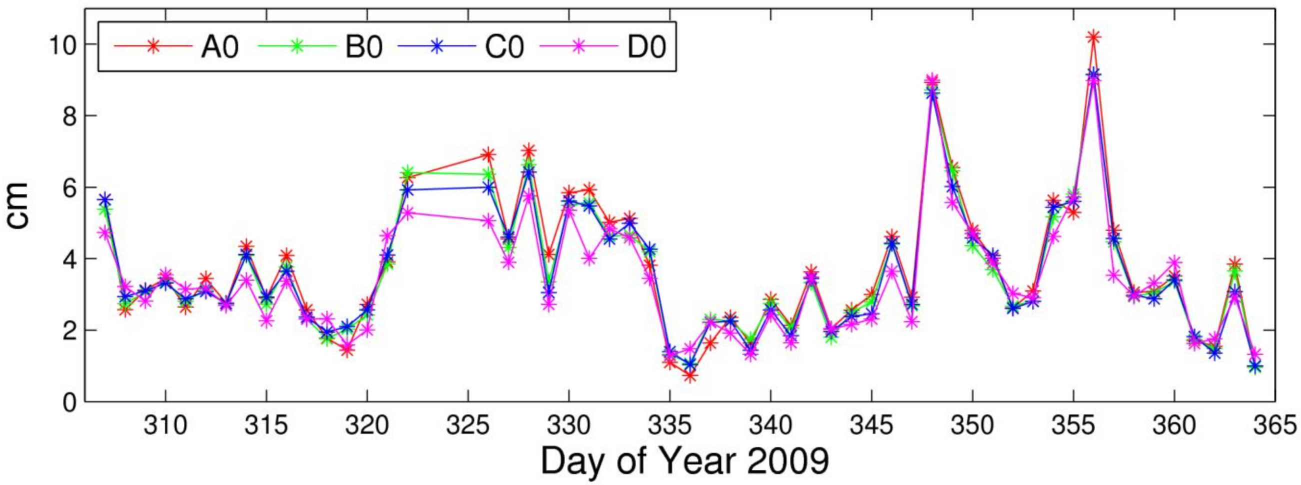

SLR validation

Mean (cm)	RMS (cm)
0.35	2.01
0.32	1.99
0.33	1.99
0.34	1.98

- 3D-position difference of orbits at midnight
- Differences compared to **A0**:
    - Use of accelerometer data, different background models (**C0**, **D0**)

=> No significant difference in the orbits

Validation of orbit quality

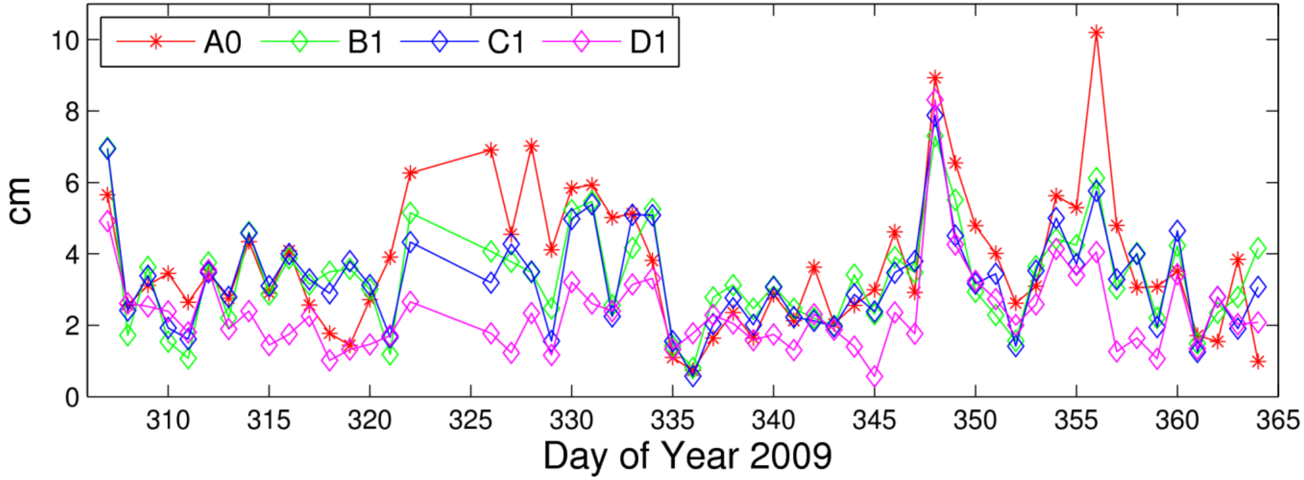

SLR validation

Mean (cm)	**RMS (cm)**
0.35	**2.01**
0.23	**2.01**
0.22	**1.98**
0.28	**1.89**

- Differences compared to **A0**:
  - Use of accelerometer data, different background models (**C1**, **D1**), tighter constraint for all components

=> **Positive impact on orbit quality: The better the background models, the better the orbits.**

Validation of orbit quality

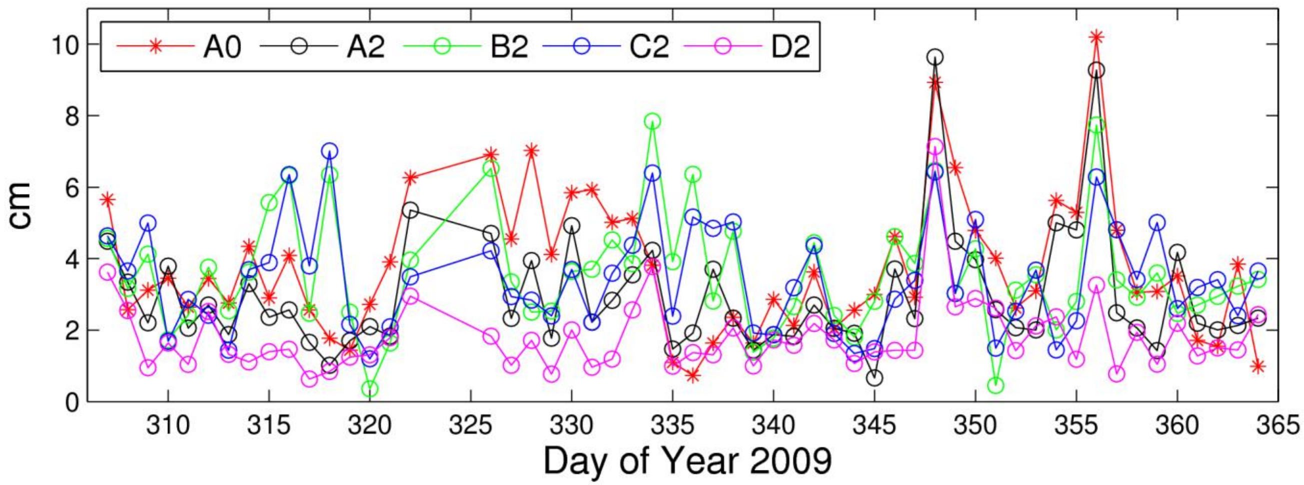

SLR validation

Mean (cm)	RMS (cm)
0.35	2.01
0.31	1.90
0.17	2.02
0.18	1.96
0.22	1.79

- Differences compared to **A0**:
  - **A2**: realistic constraints
  - **B2**,**C2**,**D2**: use of accelerometer data, different background models (**C2**, **D2**), 10% of realistic constraints

⇒**Positive impact on orbit quality: The better the background models, the better the orbits.**

⇒**10% of constraints not sufficient for B2 and C2**

Formation-flying satellites

TanDEM-X mission

Mission parameters

- Launch: June 2007 / June 2010
- Inclination: 96.5°
- Altitude: 510 km
- Distance between the two satellites: 300 – 800 m

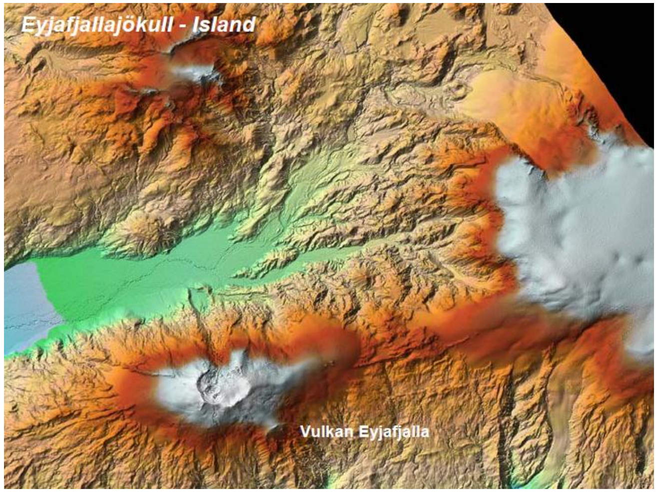

Mission goals

- global Digital Elevation Model (DEM) with a resolution of 12 m x 12 m
- vertical accuracy better than 10 m (relative accuracy better than 2 m)

TanDEM-X formation

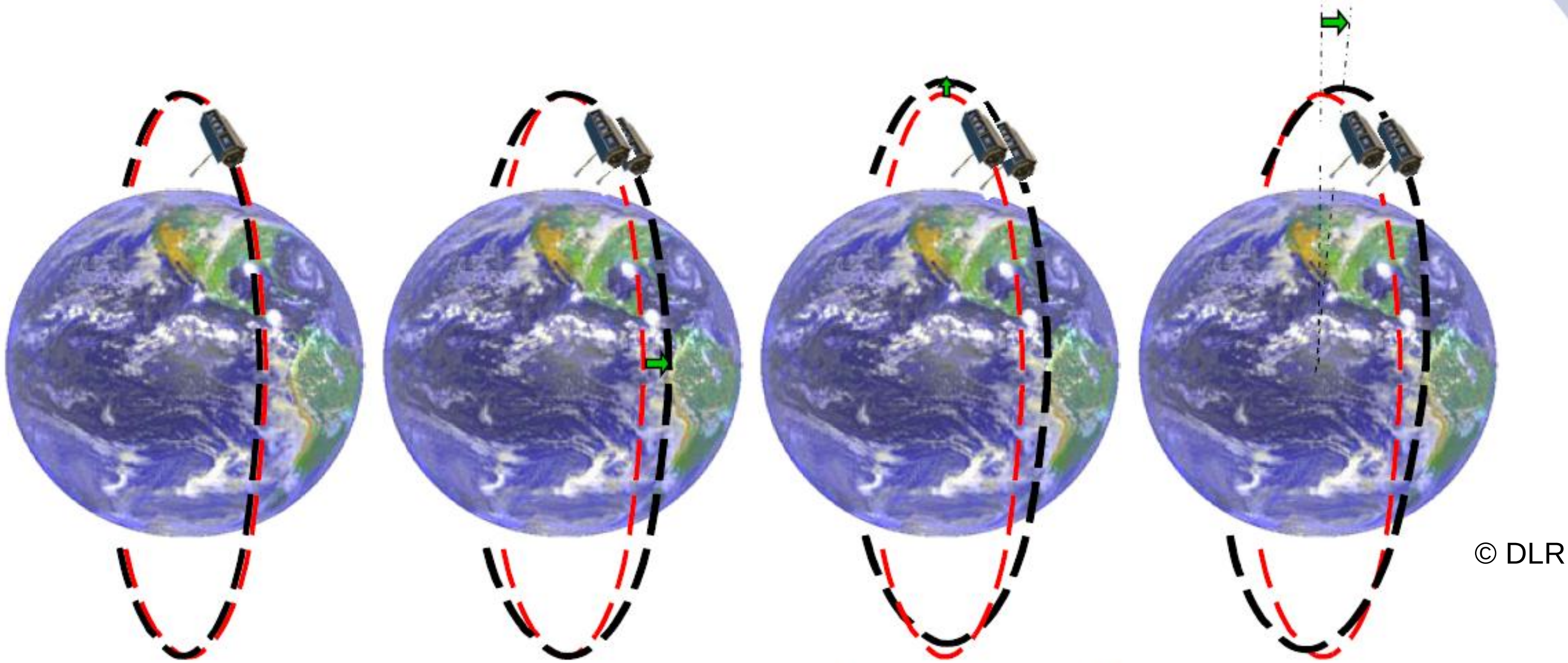

Identical orbits and identical location.

Rotate orbital plane (i.e. R.A.A.N.)
=> yields horizontal separation at equator crossings
(but orbits cross at poles)

Change eccentricity
=> causes different heights of perigee / apogee
=> yields radial separation at poles
(= safe formation)

Optionally rotate the argument of perigee
=> yields larger baselines at high latitudes

TanDEM-X formation

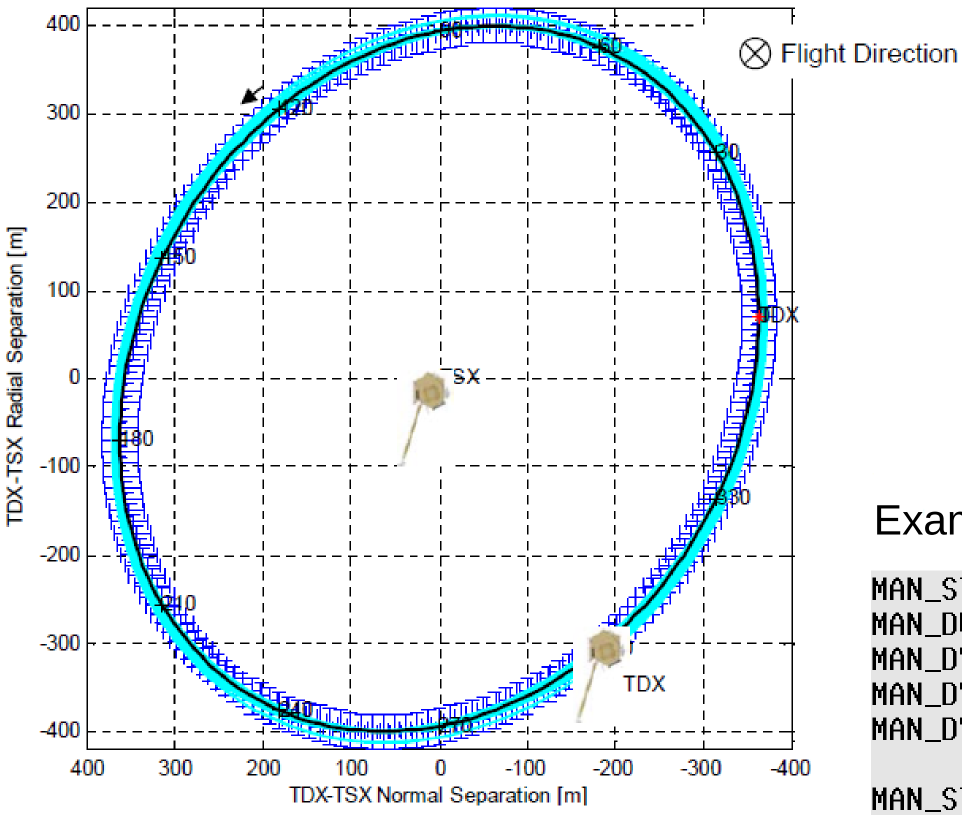

Formation is maintained by frequent maneuvers

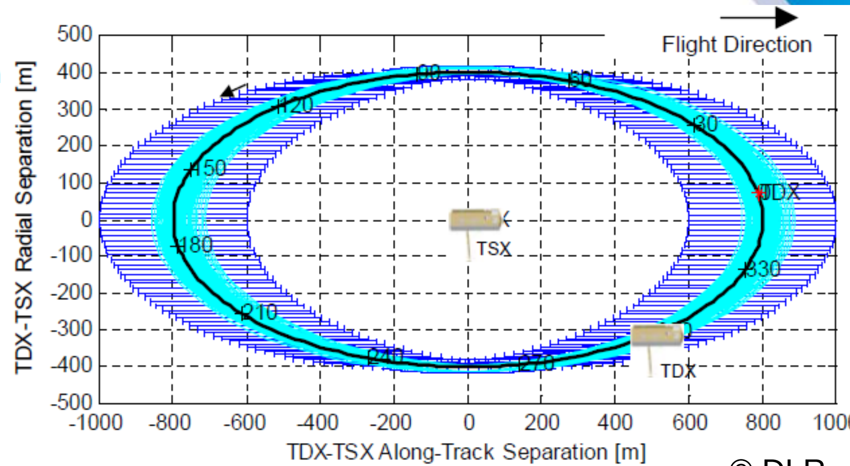

© DLR

Example of two TDX maneuvers, 0.5*U seperated

```
MAN_START          2011/01/02 23:16:35.4     % GPS Time
MAN_DURATION               96.000     % [sec]
MAN_DV_RAD              -0.000084     % [m/s]
MAN_DV_TANG             -0.005224     % [m/s]
MAN_DV_NORM              0.000366     % [m/s]

MAN_START          2011/01/03 00:04:00.3     % GPS Time
MAN_DURATION               97.165     % [sec]
MAN_DV_RAD              -0.000018     % [m/s]
MAN_DV_TANG              0.005258     % [m/s]
MAN_DV_NORM              0.000366     % [m/s]
```

TanDEM-X formation control

Formation Control Concept

- **TSX** is controlled w.r.t. TSX reference orbit
  - In-plane maneuvers: 1..5 cm/s every 20..2 days
  - Inclination maneuvers: up to 30 cm/s, 3-4 per year
- **TDX** simultaneously executes same hydrazine maneuvers as TSX (otherwise the formation breaks up)

absolute orbit control

- **TDX** performs additional cold-gas and hydrazine maneuvers
  - to maintain TDX-TSX relative motion (daily)
  - to reconfigure the formation (according to DEM acquisition plan)

relative orbit control

Baseline determination

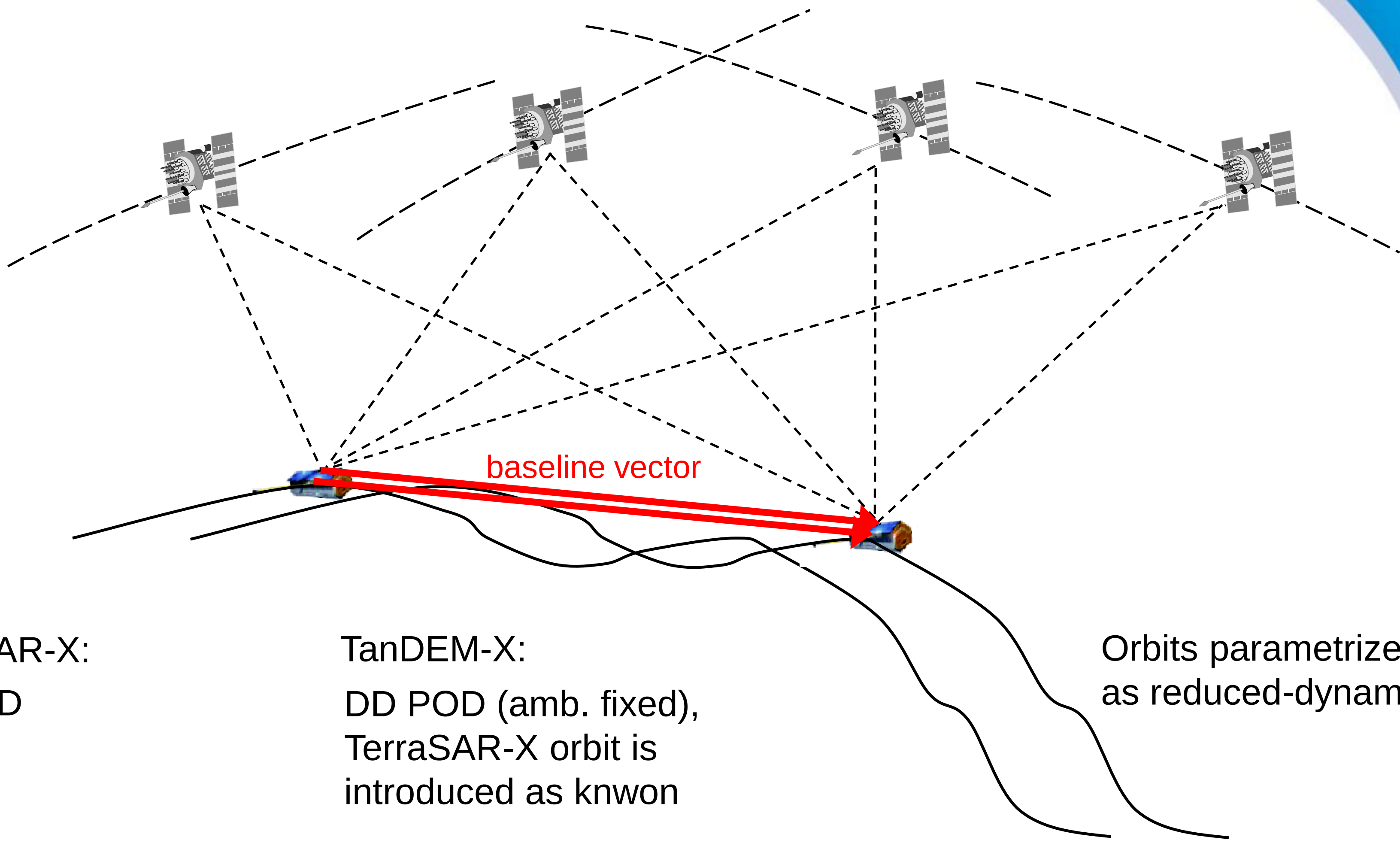

TerraSAR-X:

ZD POD

TanDEM-X:

DD POD (amb. fixed), TerraSAR-X orbit is introduced as knwon

Orbits parametrized as reduced-dynamic

Experience from GRACE

K-Band validation

- independent validation with K-band data (only line-of-sight direction, nicht absolute)
- millimeter precision confirmed (1.10 mm)
- PCV modeling important (0.81 mm)

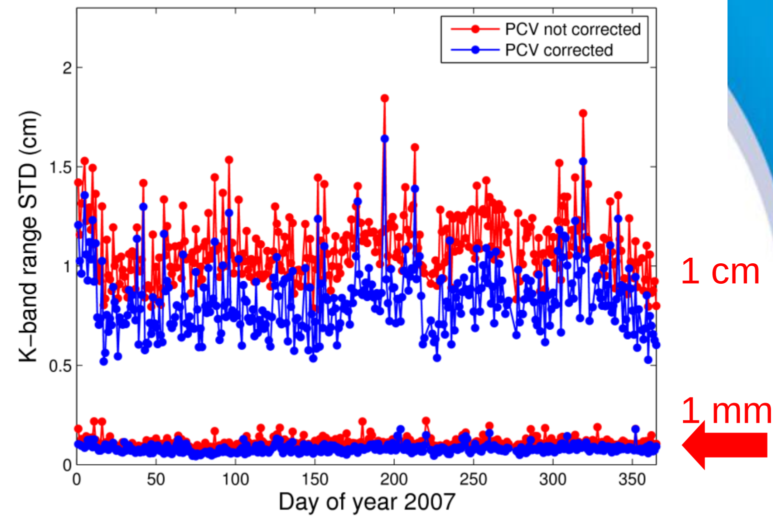

Comparison with DLR baselines

- scatter (STD) in the millimeter range (0.80, 1.04 und 1.54 mm)
- biases (mean) not (?) very large (0.95, -0.85 und 2.04 mm)
- cross-track direction is critical

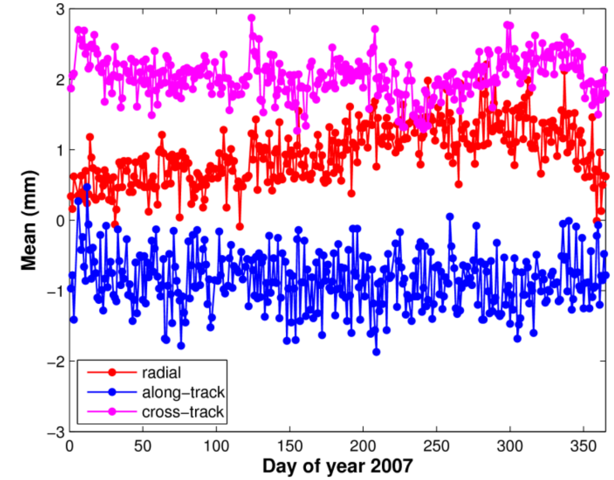

TanDEM-X inter-agency comparison

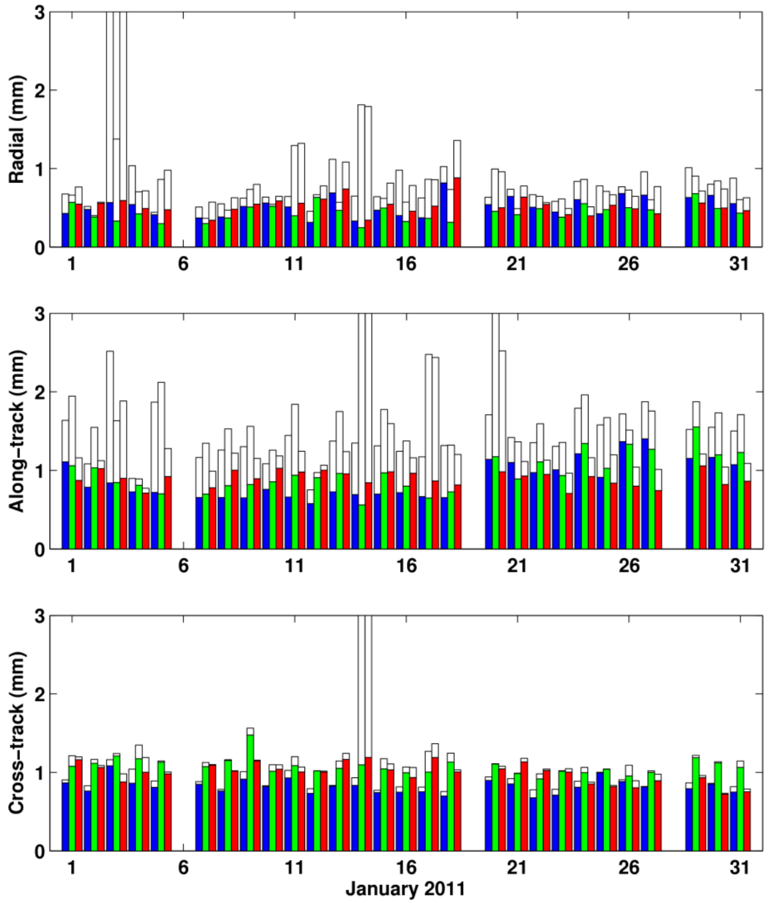

STD per day (in mm)

Dual-frequency solutions:

GFZ Helmholtz-Zentrum Potsdam — DLR Deutsches Zentrum für Luft- und Raumfahrt e.V. in der Helmholtz-Gemeinschaft — AIUB

Std (mm)	radial	along-track	cross-track
GFZ - DLR	0.5 (0.7)	0.8 (1.4)	0.8 (0.9)
GFZ - AIUB	0.4 (0.7)	0.9 (1.7)	1.0 (1.1)
AIUB - DLR	0.5 (0.8)	0.9 (1.2)	1.0 (1.1)

Mean (mm)	radial	along-track	cross-track
GFZ - DLR	-0.2	-0.4	-0.4
GFZ - AIUB	-0.1	-1.2	-1.1
AIUB - DLR	-0.1	0.7	0.7

Statistics for one month (median in mm)

=> Mission requirements are 1 mm (1D RMS)

Dual-frequency vs. single-frequency

Median values (in mm) of daily STD's for one month of reduced-dynamic baseline differences between AIUB und DLR for different observables:

Comparison	Radial	Along-track	Out-of-plane
L1(C) & L2(P)	0.5	0.9	1.0
L1(P) & L2(P)	0.5	0.9	0.9
L1(C)	0.3	0.4	0.8

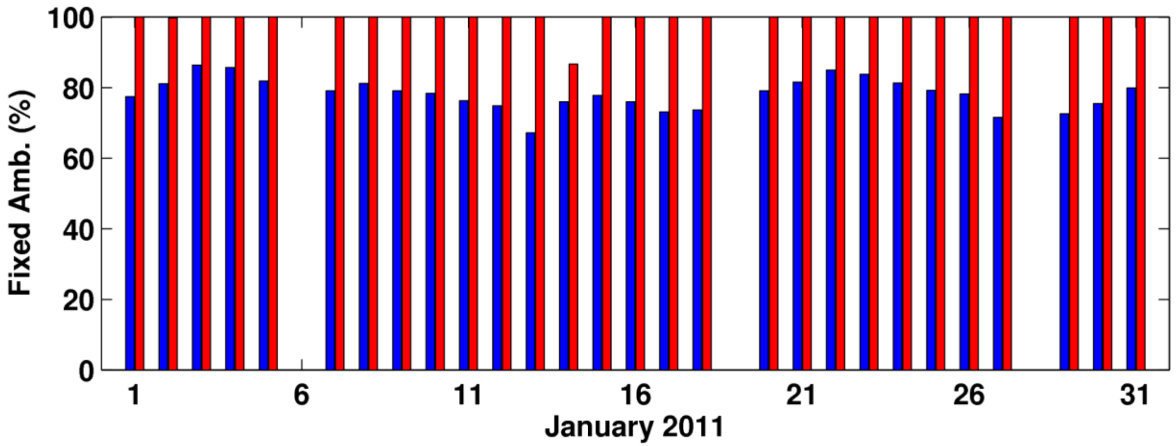

78% of the wide-lane ambiguities fixed (L1(C) & L2(P))

100% of the L1 ambiguities fixed (L1(C))

Differential single-frequency PCVs

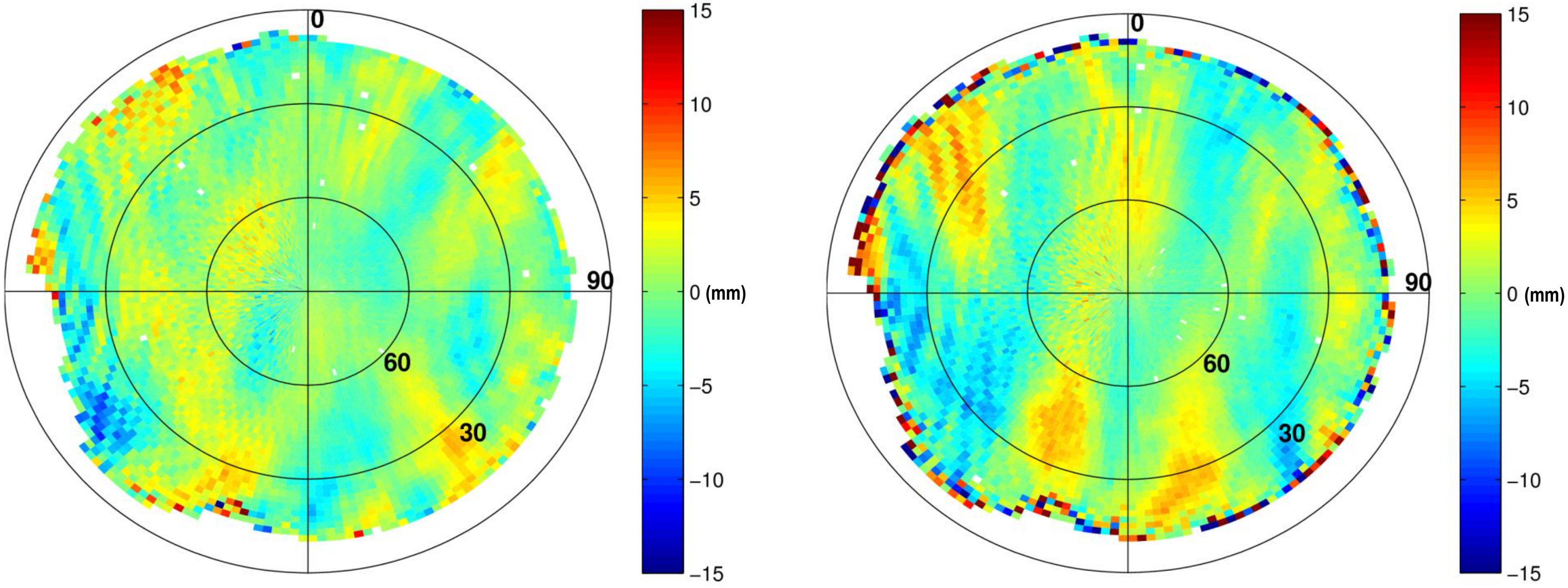

L1(C) L2(P)

For single-frequency baseline determination **differential PCVs** are needed, because single-satellite solutions (and thus single-satellite PCVs) cannot be easily generated with the required accuracy

TanDEM-X inter-agency comparisons

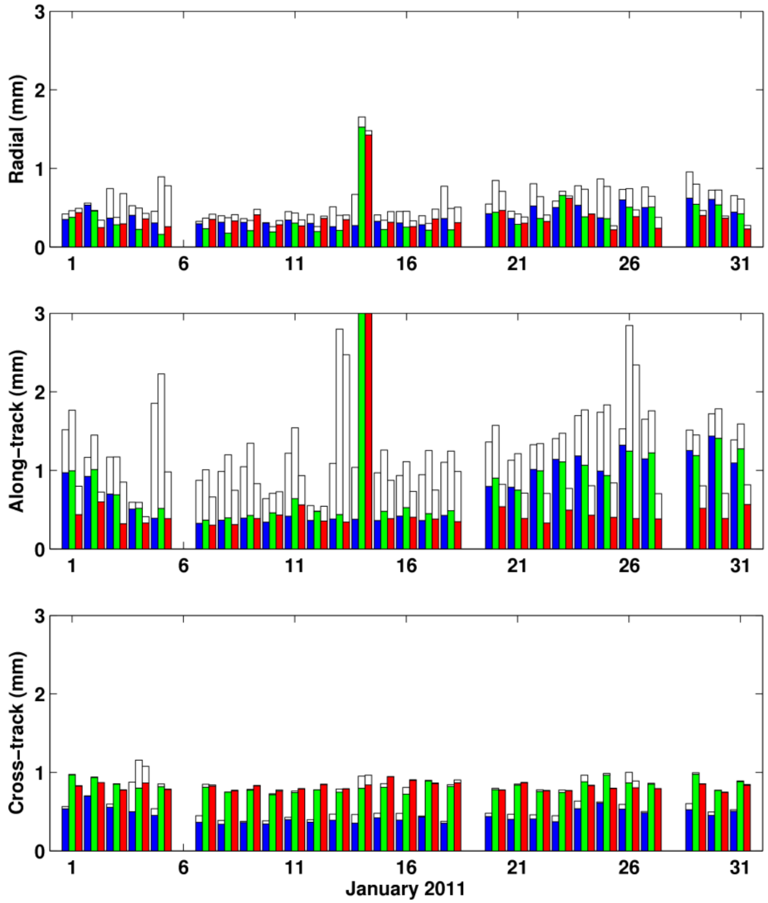

STD per day (in mm)

Single-frequency solutions:

Std (mm)	radial	along-track	cross-track
GFZ - DLR	0.4 (0.5)	0.6 (1.2)	0.4 (0.5)
GFZ - AIUB	0.3 (0.5)	0.7 (1.4)	0.8 (0.9)
AIUB - DLR	0.3 (0.4)	0.4 (0.8)	0.8 (0.8)

Mean (mm)	radial	along-track	cross-track
GFZ - DLR	-0.1	-0.8	-0.1
GFZ - AIUB	-0.2	-1.2	0
AIUB - DLR	0.2	0.3	0.8

Statistics for one month (Median in mm)

From orbits to the gravity field

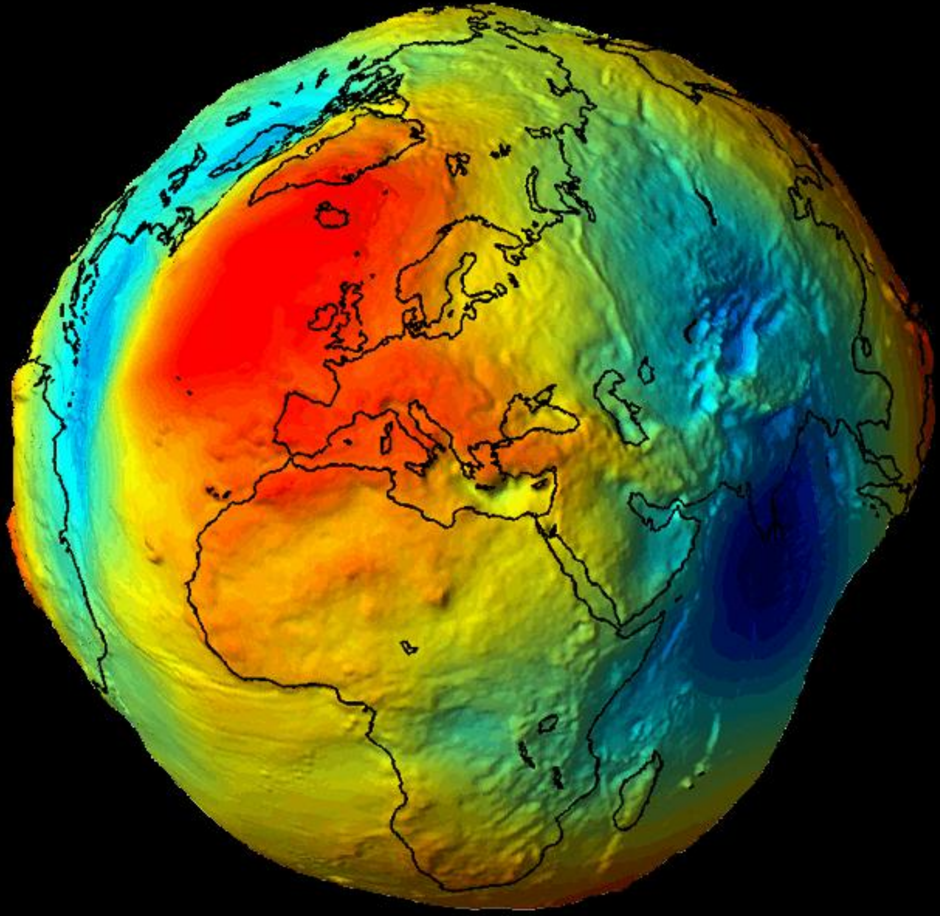

From orbits to the gravity field

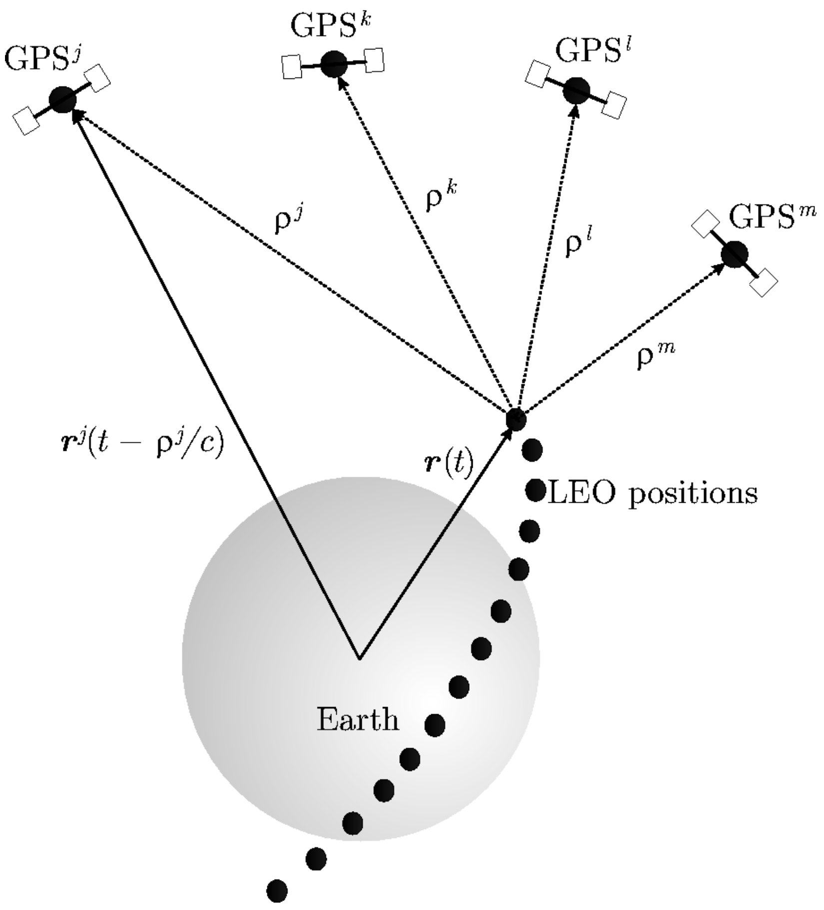

- **Kinematic positions contain independent information about the long-wavelength part of the Earth's gravity field**
- **1-sec kinematic positions serve as pseudo-observations together with covariance information to set-up an orbit determination problem, which also includes gravity field parameters**
- **Non-gravitational forces are absorbed by empirical parameters in the course of the generalized orbit determination problem, accelerometer data are not used**
- **Gravity field coefficients are either solved for up to d/o 120 or d/o 160 in the following slides without applying any regularization**

From orbits to the gravity field

Kinematic Orbit Positions
Pseudo-Observations with Covariance Information

Accelerometer Data
(optional**)**

Set-up of an Orbit Determination Problem by Least-Squares
- **computation of the observation equations for each daily arc by numerical integration**
  (global parameters: SH coefficients; arc-specific parameters, e.g., initial conditions and accelerations)
- **construction of the normal equations for each daily arc**

Manipulation of Normal Equation Systems
- **manipulation and subsequent pre-elimination of arc-specific parameters**
  (e.g., constraining or downsampling of accelerations)
- **accumulation of daily normal equations into monthly and annual systems**
- **regularization of SH coefficients**
  (not used**)**
- **inversion of the resulting normal equation systems**

Experience from GRACE

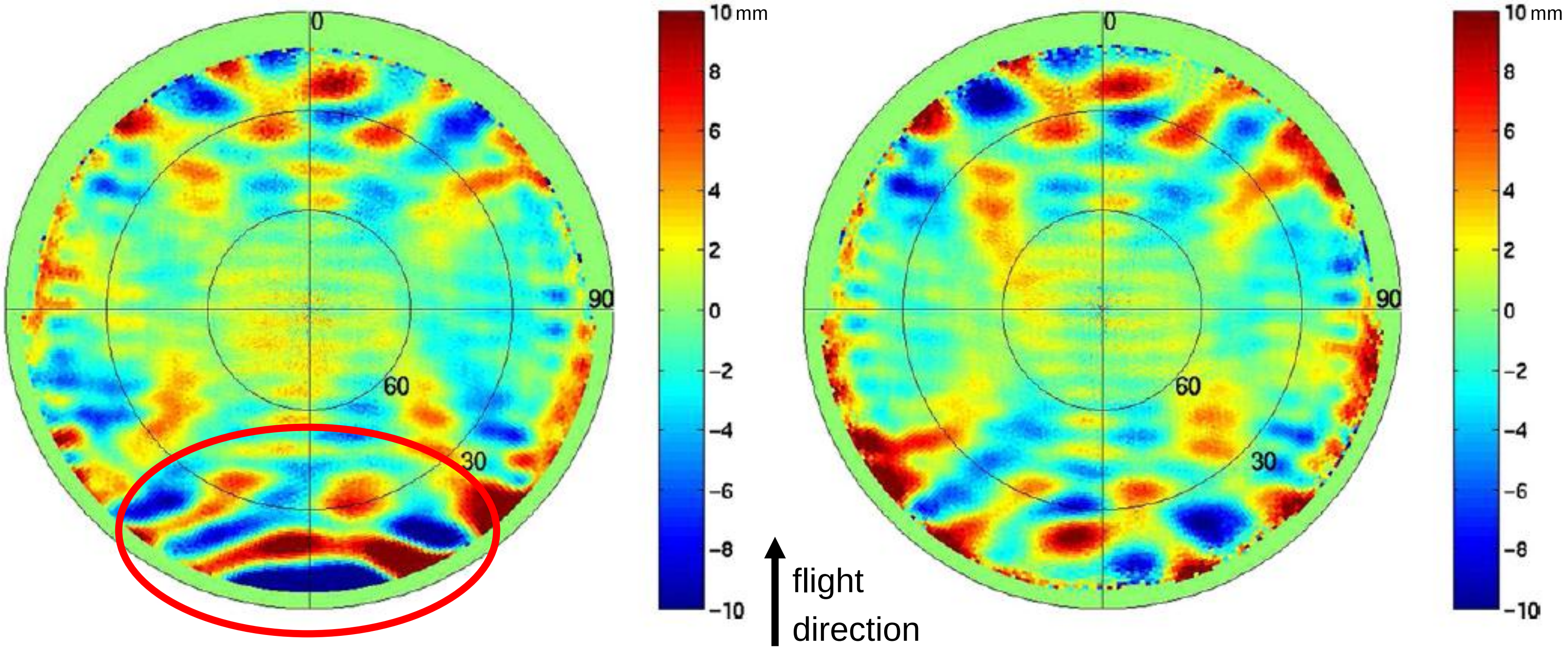

GRACE A
(occultation antenna switched on)

GRACE B

Impact on the gravity field

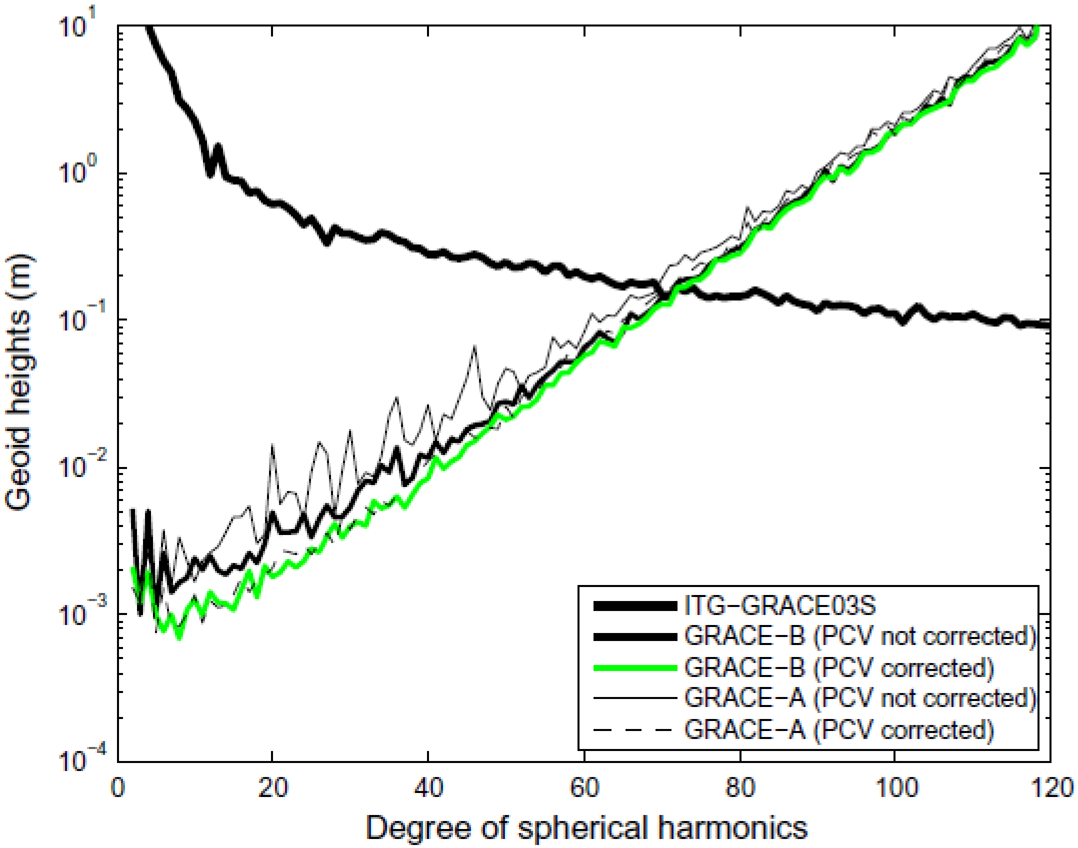

- Very similar results for GRACE A and for GRACE B when taking PCV corrections for kinematic POD into account
- More pronounced degradation for GRACE A when ignoring PCV corrections for kinematic POD (occultation antenna on)
- Impact visible up to relatively high degree and orders

PCV modeling is very important for GPS-based gravity field recovery

What's about GOCE?

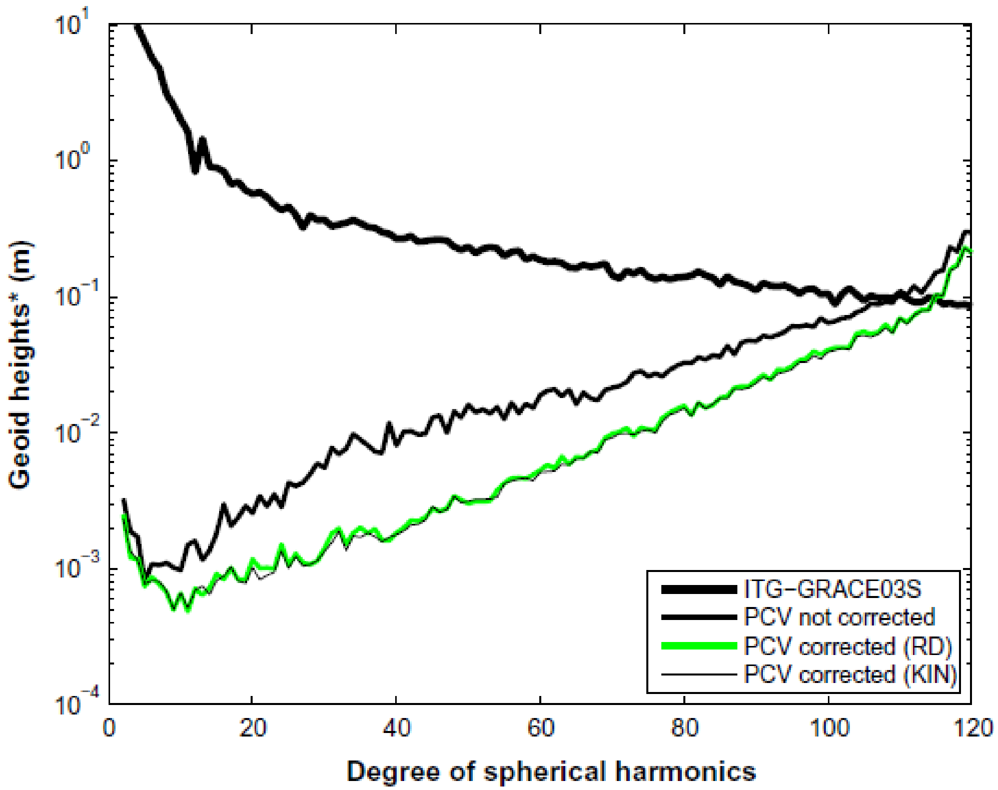

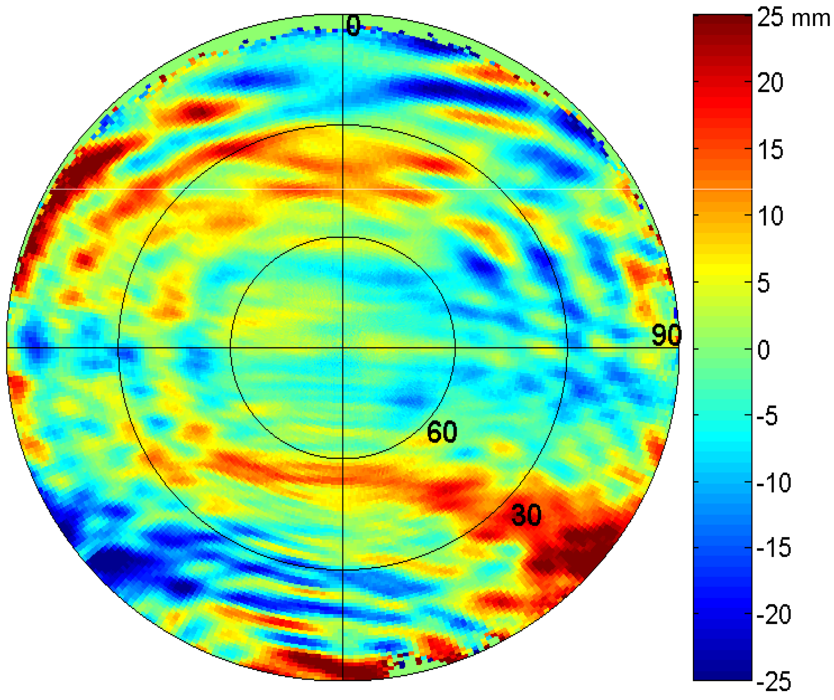

PCV modeling is even more important than for GRACE due to the more complicated patterns caused by the GOCE **helix antenna**

Impact of polar gap

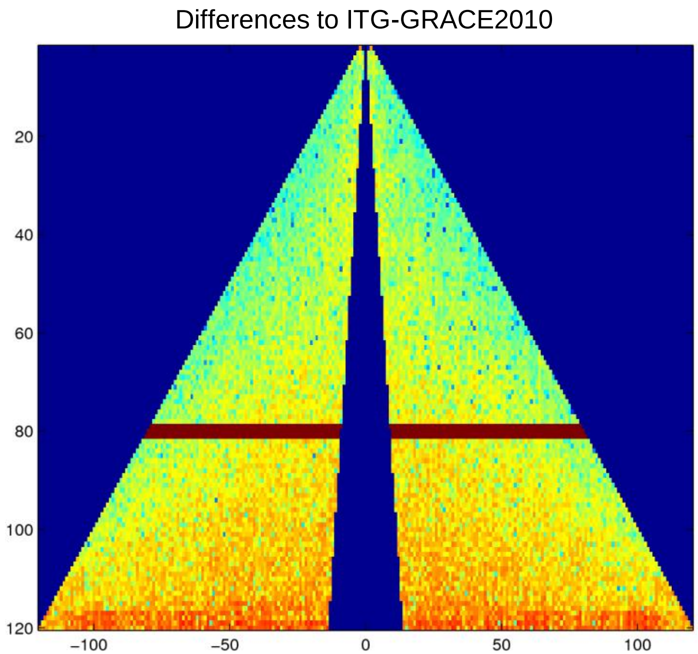

$$\delta d_i \doteq \sqrt{\sum_{m=0}^{i} \left(\Delta \bar{C}_{i,m}^2 + \Delta \bar{S}_{i,m}^2 \right)}$$

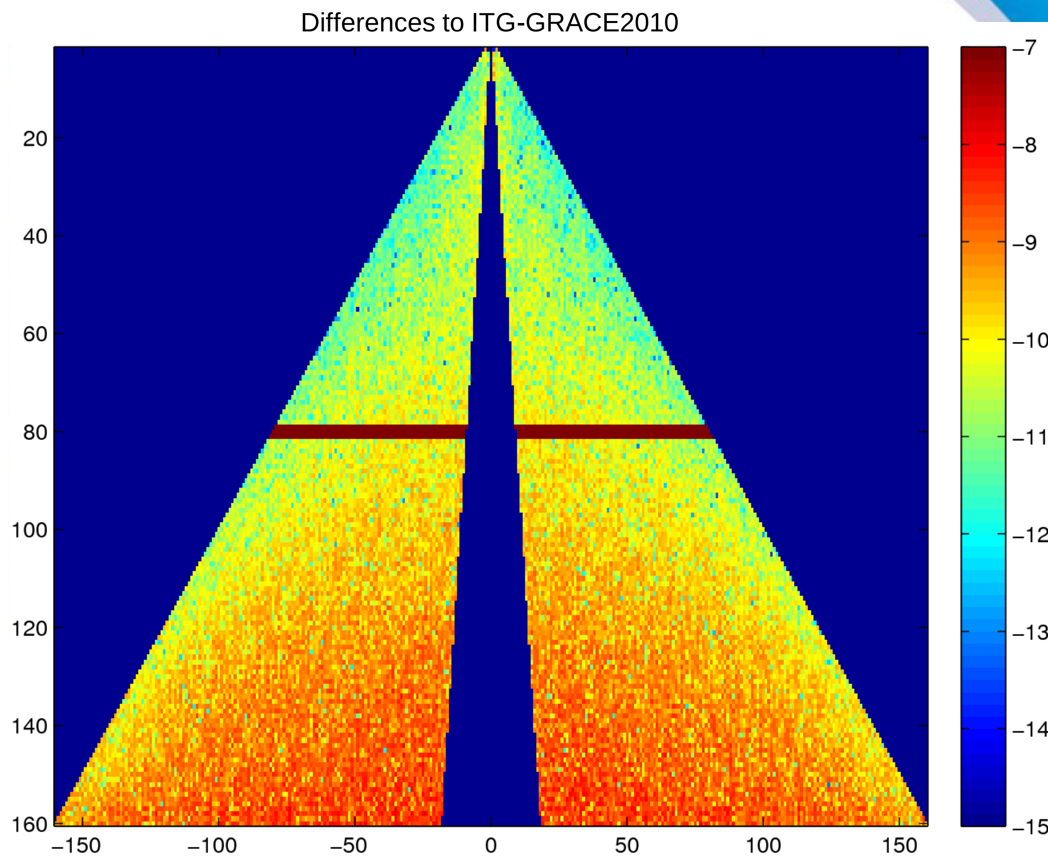

- δd_i is dominated by zonal and near-zonal terms, degradation depends on max. d/o
- => exclusion according to the rule of thumb by van Gelderen & Koop

Solution characteristics

Differences to ITG-GRACE2010

unfiltered, d/o 100

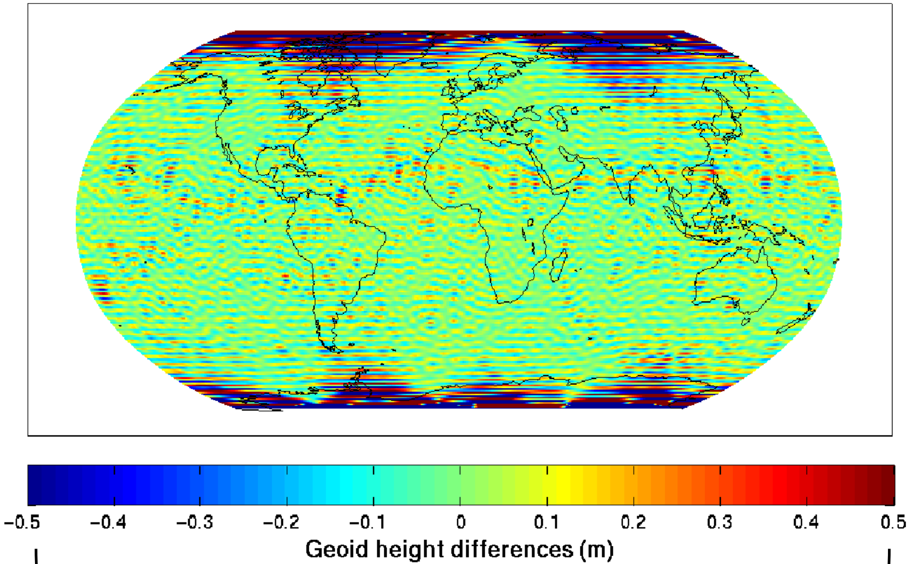

300 km Gauss-filtered

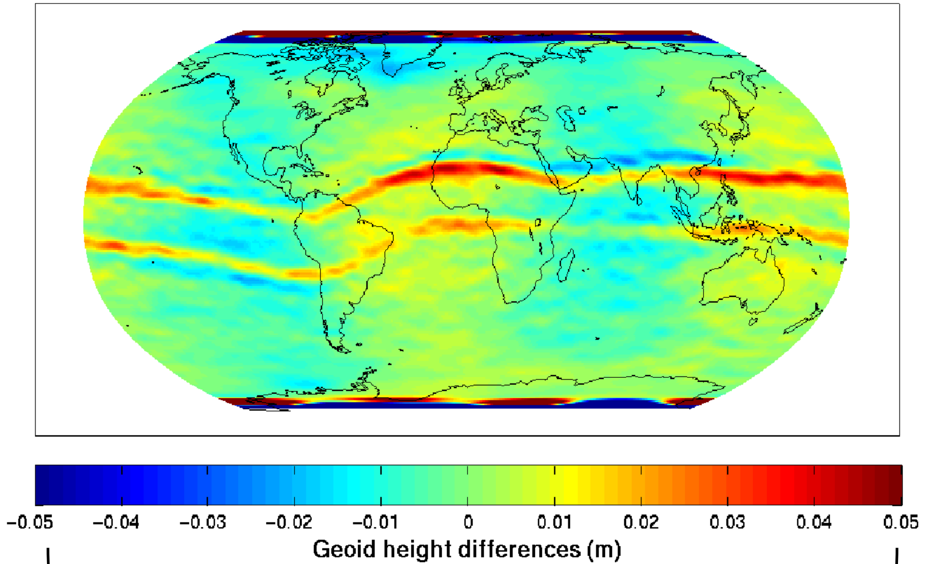

increased noise over polar regions

magnetic equator visible

	2009:	**2009-10:**	**2009-11:**
RMS (unfiltered):	113.3 cm	76.1 cm	38.9 cm
RMS (filtered):	4.9 cm	3.1 cm	2.0 cm

Combination with CHAMP

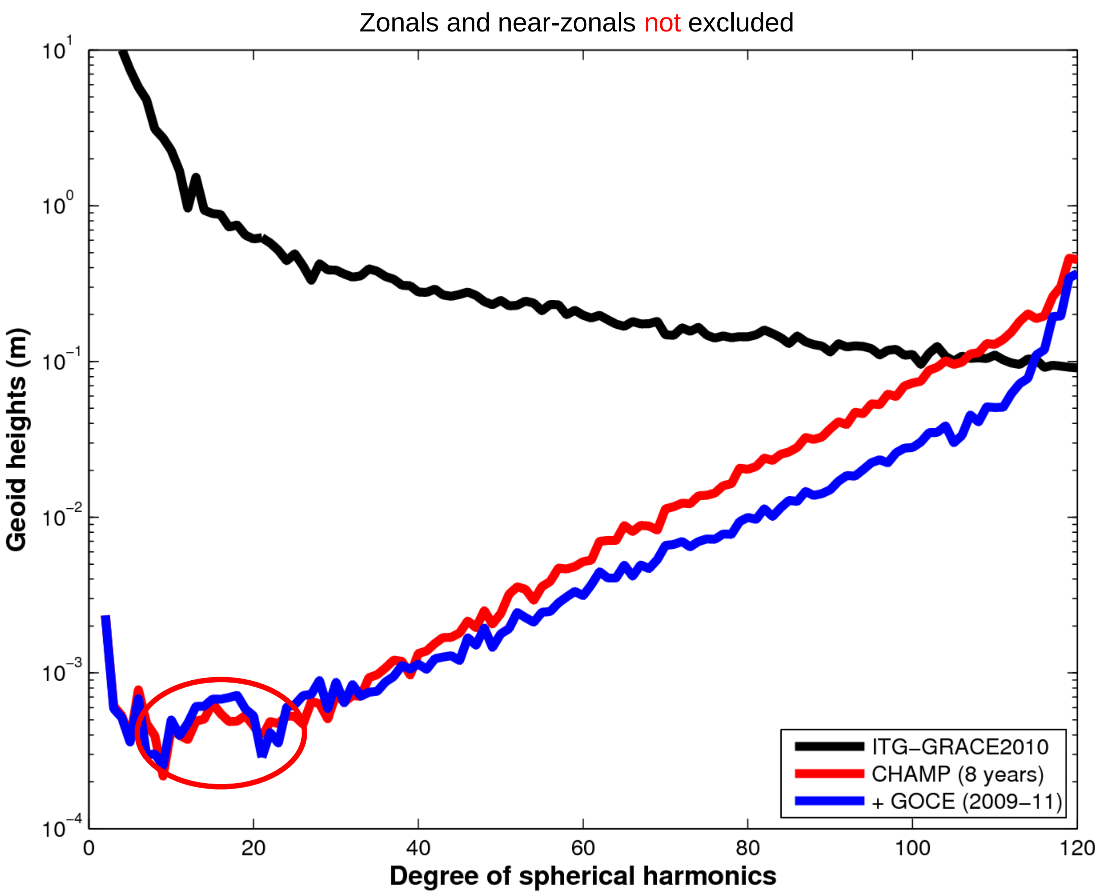

- **Down-weighting of the GOCE normal equations is required due to an only marginal contribution of the 1-sec data wrt 5-sec sampled data**
- **No degradation due to the polar gap in the combined solution**
- **Small degradation when including the most recent GOCE data**

Contribution to gradiometer solution

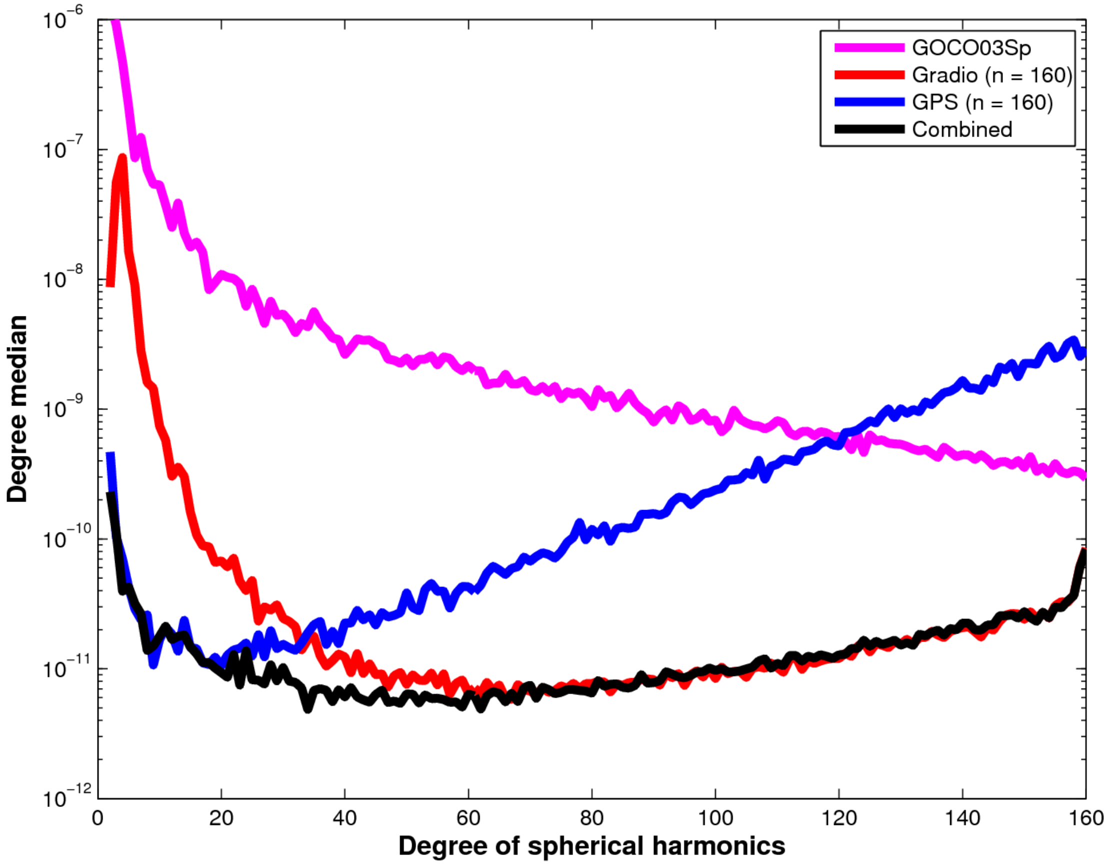

- **8 months of GPS and gradiometer data used**
- **GPS dominates the combination up to about degree 20 and contributes up to about degree 70**
- **No omission artifacts in the combined solution when using GPS beyond degree 120. No need to artificially down-weight the GPS contribution**

Thank you for your attention

Literature

Beutler, G., A. Jäggi, L. Mervart, U. Meyer (2010): The celestial mechanics approach: theoretical foundations. *Journal of Geodesy*, 84(10), 605-624, doi: 10.1007/s00190-010-0401-7

Bock, H., A. Jäggi, D. Švehla, G. Beutler, U. Hugentobler, P. Visser (2007): Precise orbit determination for the GOCE satellite using GPS. *Advances in Space Research*, 39(10), 1638-1647, doi: 10.1016/j.asr.2007.02.053

Bock, H., A. Jäggi, U. Meyer, P. Visser, J. van den IJssel, T. van Helleputte, M. Heinze, U. Hugentobler (2011): GPS-derived orbits for the GOCE satellite. *Journal of Geodesy*, 85(11), 807-818, doi: 10.1007/s00190-011-0484-9

Bock, H., A. Jäggi, U. Meyer, R. Dach, G. Beutler (2011): Impact of GPS antenna phase center variations on precise orbits of the GOCE satellite. *Advances in Space Research*, 47(11), 1885-1893, doi: 10.1016/j.asr.2011.01.017.

Jäggi, A., U. Hugentobler, G. Beutler (2006): Pseudo-stochastic orbit modeling techniques for low-Earth satellites. *Journal of Geodesy*, 80(1), 47-60, doi: 10.1007/s00190-006-0029-9

Literature

Jäggi, A. (2007): Pseudo-Stochastic Orbit Modeling of Low Earth Satellites Using the Global Positioning System. *Geodätisch-geophysikalische Arbeiten in der Schweiz*, 73, Schweizerische Geodätische Kommission, available at http://www.sgc.ethz.ch/sgc-volumes/sgk-73.pdf

Jäggi, A., R. Dach, O. Montenbruck, U. Hugentobler, H. Bock, G. Beutler (2009): Phase center modeling for LEO GPS receiver antennas and its impact on precise orbit determination. *Journal of Geodesy*, 83(12), 1145-1162, doi: 10.1007/s00190-009-0333-2

Jäggi, A., H. Bock, L. Prange, U. Meyer, G. Beutler (2011): GPS-only gravity field recovery with GOCE, CHAMP, and GRACE. *Advances in Space Research*, 47(6), 1020-1028, doi: 10.1016/j.asr.2010.11.008

Jäggi, A., O. Montenbruck, Y. Moon, M. Wermuth, R. König, G. Michalak, H. Bock, D. Bodenmann (2012): Inter-agency comparison of TanDEM-X baseline solutions. *Advances in Space Research*, 50(2), 260-271, doi: 10.1016/j.asr.2012.03.027.

Montenbruck O., R. Neubert (2011): Range Correction for the CryoSat and GOCE Laser Retroreflector Arrays. *DLR-GSOC TN 11-01*, Deutsches Zentrum für Luft- und Raumfahrt, Oberpfaffenhofen, Germany.

Literature

Montenbruck, O., M. Wermuth, R. Kahle (2011): GPS Based Relative Navigation for the TanDEM-X Mission - First Flight Results. *Navigation - Journal of the Institute of Navigation*, 58(4), 293-304

Floberghagen, R., M. Fehringer, D. Lamarre, D. Muzi, B. Frommknecht, C. Steiger, J. Piñeiro, A. da Costa (2011): Mission design, operation and exploitation of the gravity field and steady-state ocean circulation explorer mission. Journal of Geodesy, 85(11), 749-758, doi: 10.1007/s00190-011-0498-3

Švehla, D., M. Rothacher (2004): Kinematic Precise Orbit Determination for Gravity Field Determination, in *A Window on the Future of Geodesy*, edited by F. Sanso, pp. 181-188, Springer, doi: 10.1007/b139065

Visser, P., J. van den IJssel, T. van Helleputte, H. Bock, A. Jäggi, G. Beutler, D. Švehla, U. Hugentobler, M. Heinze (2009): Orbit determination for the GOCE satellite, *Advances in Space Research*, 43(5), 760-768, doi: 10.1016/j.asr.2008.09.016